Università degli Studi di Ferrara

DOTTORATO DI RICERCA IN
FARMACOLOGIA E ONCOLOGIA MOLECOLARE

CICLO XXVII

COORDINATORE Prof. Cuneo Antonio

Analysis of the anti-leukemic activity of sodium dichloroacetate

Settore Scientifico Disciplinare BIO/16

Dottorando
Dott. Agnoletto Chiara

Tutore
Prof. Zauli Giorgio

Correlatore
Prof.ssa Secchiero Paola

Anni 2012/2014

Table of contents

INTRODUCTION pg 1

B chronic lymphocytic leukemia pg 1

Prognostic markers in B-CLL pg 2

Current management of chronic lymphocytic leukemia pg 5

Metabolic transformation in cancer pg 8

Metabolism in chronic lymphocytic leukemia pg 10

Targeting aerobic glycolysis in chronic lymphocytic leukemia pg 11

The oncosuppressor TP53: role in metabolic transformation pg 12

Targeting p53 with Nutlin-3 as potential therapeutic option for B-CLL pg 16

OBJECTIVES pg 18

METHODS pg 19

Primary B-CLL patient samples and B leukemic cell lines pg 19

Culture treatments, assessment of cell viability, apoptosis, cell cycle profile and Senescence pg 20

Assessment of mitochondrial alterations pg 20

Western blot analyses pg 21

Bi-dimensional gel electrophoresis (2-DE) and immunoblotting pg 21

Proteomic profiling pg 22

cDNA microarray and RT-PCR analyses pg 23

RNA analyses pg 24

Transfection experiments pg 24

Statistical analysis and assessment of the effect of combination treatment pg 25

RESULTS pg 26

DCA promotes cytotoxicity in primary B-CLL patient derived cells, but not in normal peripheral blood cells pg 26

DCA activates the p53 pathway in $p53^{wild\text{-}type}$ B leukemic cell lines pg 29

DCA plus Nutlin-3 combination exhibits a potent synergistic anti-leukemic activity pg 32

Role of p21 induction in DCA and DCA+Nutlin-3 induced cytotoxicity in leukemic cells pg 34

DCA promotes comparable cytotoxicity in $p53^{wild\text{-}type}$ and $p53^{mutated}$ B-CLL patient cells pg 37

DCA effects on HL-60 apoptosis, cell cycle and mitochondrial energy metabolism transcriptomic profile pg 42

DCA induces the transcription of p21 in both $p53^{wild\text{-}type}$ and $p53^{mutated/null}$ leukemic cells pg 45

DCA effects on HL-60 proteomic profile pg 46

Role of ILF3-p21 axis in DCA induced cytotoxicity pg 50

DISCUSSION pg 53

Conclusions pg 55

REFERENCES pg 56

LIST OF PUBLICATIONS IN PhD pg 66

Introduction

B chronic lymphocytic leukemia

B chronic lymphocytic leukemia (B-CLL) is the adult leukemia with the highest incidence in Western countries; more than 15.000 newly diagnosed cases and 4.500 deaths are currently estimated yearly. It is characterized by the clonal proliferation and accumulation of differentiated CD5+/CD23+ B lymphocytes in the peripheral blood and lymphoid organs [**1,2**]. B-CLL is an heterogeneous disorder in terms of progression, therapeutic response and outcome despite a common diagnostic immunophenotype (surface expression of CD19+, CD20+^{dim}, CD5+, CD23+ and sIgM^{dim}) [**2**]. The leukemic transformation is initiated by specific genomic alterations, in particular deletions on the long arm of chromosome 13 [del(13q14)]. Additional aberrations of the long arm of chromosome 11 [del(11q)], of the short arm of chromosome 17 [del(17p)] and trisomy of chromosome 12 seem to occur later in the course of the disease and predict a worse outcome [**3-5**].

The diagnosis of CLL is currently based on clinical analyses of lymphocyte morphology and the presence of >5x10^9/l circulating clonal B cells with the specific immunophenotype persisting for >3 months [**1**]. A recommended scoring system allocates one point each for the expression of weak surface membrane immunoglobulins, CD5, CD23 and absent or low expression of CD79b and FMC7. Using this system, 92% of B-CLL cases score 4 or 5, 6% score 3 and 2% score 1 or 2 [**1**]. Frequently at diagnosis patients present lymphadenopathy and systemic symptoms such as tiredness, night sweats and weight loss; signs of advanced stages of leukemia include impaired function of normal bone marrow elements, such as anemia and leucopenia, with higher susceptibility to infections [**1**]. 5-15% of B-CLL patients develop diffuse large B cell lymphoma (Richter syndrome) or, less frequently, Hodgkin lymphoma, either pre- or post-therapy. Clinical features suggestive of transformation include bulky (>5 cm) lymphoadenopathy, rapid nodal enlargement, extranodal disease, the development of B symptoms and marked elevation of lactate dehydrogenase (LDH). Moreover, autoimmune complications are common in B-CLL, occurring in 10-20% of patients and they target almost exclusively blood cells, in particular erythrocytes. The diagnosis of autoimmune

haemolytic anemia is based on the presence of an isolated reduction in haemoglobin with positive direct antiglobulin test, a rise in reticulocyte count, bilirubin and LDH and a reduction in serum haptoglobins [**1**]. Whereas the course of disease is indolent in some patients, it is steadily progressive in approximately half of patients, leading to substantial morbidity and mortality [**2**]. The variable clinical course of B-CLL is due, at least in part, to the disease's immunogenetic and molecular heterogeneity [**2**].

Numerous clinical and laboratory parameters have been developed to predict prognosis. Clinical staging systems of Binet and Rai still represent the most useful mean to determine prognosis and permit to divide patients into classes with different risk levels (Table 1) [**1**]. Commonly clinicians initiate therapeutic treatment only if patients reach advanced stages and develop a symptomatic disorder. However, while these staging systems are clinically useful, they can't predict long-term survival with high precision, especially for patients with early stage leukemia [**6**].

Table 1. Staging systems in CLL.

BINET Stage		*Features*
A		<3 Lymphoid areas*
B		≥3 Lymphoid areas
C		Haemoglobin < 100 g/l or platelet count < 100 9 109/l
RAI Stage	*Risk group*	*Features*
0	Low	Lymphocytosis only
I		Lymphadenopathy
II	Intermediate	Hepatomegaly or splenomegaly + lymphocytosis
III/IV	High	Haemoglobin < 110 g/l or platelet count < $100x10^9$/l

*The five lymphoid areas comprise: uni or bilateral cervical, axillary and inguinal lymphoid, hepatomegaly and splenomegaly.

Prognostic markers in B-CLL

The ability to predict a more aggressive disease course has improved with the use in clinical practice of tests for biologic markers (degree of somatic hypermutation in the variable region of the immunoglobulin heavy chain [IGHV] gene and expression of ZAP-70 [Z-associated protein 70] or CD38) and cytogenetic abnormalities [**3,7-10**]. High expression of both ZAP-70 or CD38 are associated with higher-risk CLL. While IGHV mutated CLL patients frequently show mild clinical features and high overall survival and progression-free survival, IGHV un-mutated CLL patients

suffer an aggressive form of the disease which may be refractory to treatment [**11**]. Moreover, although the somatic mutation status is highly associated with prognosis, recent data document that a specific heavy chain variable region genetic signature is associated with poor prognosis, independently of somatic mutational status [**12**].

Despite the relatively stable karyotype in CLL cells, genomic aberrations were recognized as important determinants of the clinical course of the disease [**13**]. In particular, chromosomal abnormalities represent strong independent predictors of prognosis in B-CLL. The most common is del(13q14.3), followed by del(11q22.3), trisomy 12, del(6q21-23) and del(17p13.1). As the sole chromosomal defect, del(13q14) is associated with a good prognosis [**5,13,14**]. In contrast, del(6q21-23), del(11q22.3), del(17p13.1), del(13q14.3) with other abnormalities, and trisomy 12 are associated with more rapid disease progression and reduced survival [**13**]. Finally, the deletions in chromosome 17p, containing the TP53 gene, and chromosome 11q, containing the ATM gene, represent the most important independent cytogenetic markers of poor prognosis [**5**].

Still, even with these advances, prediction of the disease course is not highly reliable, and the genomic events that dictate the initiation and heterogeneous evolution of B-CLL remained partially unknown [**15,16**]. Next-generation sequencing (NGS) studies have revealed previously unrecognized genetic lesions, uncovering recurrent somatic gene mutations that occur in B-CLL cells in parallel to the above-mentioned structural genomic aberrations [**3-5,16,17**]. These studies described about 1,000 somatic variants per patient, evidencing a marked genetic heterogeneity of the disease, with a relatively large number of genes recurrently mutated at low frequency and only a few genes mutated in more than 10% of the patients [**5,10,18,19**].

Among genes that are mutated at significant frequencies, TP53, ATM, MYD88 and NOTCH1 have been described previously in chronic lymphocytic leukemia [**3,5,20-24**]. TP53 mutations were detected in 15% of patients and most of them in CLL represent missense substitutions affecting the structural DNA-binding domain (DBD) of p53 protein (codons 175, 179, 248, 273, and 281) that is critical for its tumor-suppressor activity [**5,21,22,25**], with one mutation out of 105 cases in Quesada et al. [**4**] and 15 mutations out of 91 cases in Wang et al. [**5**]. The proportion of patients with a sole TP53 mutation [without del(17p)] vary from 3% to 4% among cohorts at diagnosis or before first therapy [**21**] to 12% in fludarabine-refractory CLL [**26**]. A prognostic impact of TP53 mutations in B-CLL has been suggested in a number of reports [**21**]. Patients with defective p53 have a significantly lower response rate to therapy and a short-progression-free survival [**22**]. Indeed, TP53 mutation and related alterations have been associated with disease progression and chemorefractoriness in B-CLL [**27,28**]. Additionally, although TP53 mutations in naïve B-CLL were usually considered a rare

(<5%) event [**29,30**], a recent study performed using the ultra-deep next generation sequencing technology demonstrated that very small TP53 mutated subclones (minor than 20%) are present in 9% of newly diagnosed B-CLL patients [**31**]. Of note, patients harboring small TP53 mutated subclones showed the same clinical phenotype and poor overall survival as patients carrying clonal TP53 lesions [**31**]. In addition, the percentage of TP53 mutations dramatically increases up to >30% after relapsed chemotherapy [**32**]. According to the revised National Cancer Institute (NCI) Working Group/International Workshop on Chronic Lymphocytic Leukemia guidelines for B-CLL, patients with del(17p) should be offered investigative clinical protocols or should be listed for allogeneic stem-cell transplantation [**22**].

9% of patients with B-CLL present mutations in ATM [**5,20**]. The ataxia telangiectasia mutated (ATM) protein kinase acts upstream of the p53 oncoprotein and coordinates an integrated cellular response to DNA double-strand breaks through phosphorylation of multiple target proteins. This results in the interruption of the cell cycle and either DNA repair or activation of apoptosis [**20,33**]. The ATM tumor suppressor gene is located within the minimally deleted region on chromosome 11q. Deletions of chromosome 11q were associated with a severe clinical phenotype and reduced overall survival in B-CLL. ATM mutations were associated with un-mutated IGVH genes and they provided independent prognostic information on multivariate analysis [**20**].

In addition, recurrent mutations in the myeloid differentiation primary response gene 88 (MYD88) were also identified in 10% of CLL patients [**5**]. This protein participates in the signalling pathways of interleukin-1 and Toll-like receptors during the immune response [**34**]. The missense mutations are localized within the interleukin-1 receptor–TLR domain [**4,24**], and they were documented to activate this proto-oncogene, promoting the duplication of tumour cells and protecting from apoptosis [**24,35,36**]. Patients with MYD88-mutated CLL were diagnosed at a younger age and with a more advanced clinical stage [**3**].

Finally, NOTCH1 mutations affect 5–10% of newly diagnosed B-CLL cases, with their prevalence increasing to 15–20% in progressive or relapsed patients [**23**]. NOTCH1 is constitutively expressed by B-CLL cells, where it increases cell survival and induces apoptosis resistance [**37-39**]. A recurrent mutation is due to the deletion of a CT dinucleotide (p.P2515Rfs*4), generating a truncated protein which is predicted to result in NOTCH1-impaired degradation and stabilizing effect on the NOTCH1 signaling pathway [**3,16**]. Indeed both the canonical and non-canonical NOTCH1 pathways are constitutively upregulated in NOTCH1-mutated patients [**16**]. NOTCH1-mutated patients had a more advanced clinical stage at diagnosis, more adverse biological features and an overall survival that was significantly shorter than those with wild-type NOTCH1 [**3,10,23,38**].

Interestingly, on a clinical perspective, among the novel genes that are recurrently mutated in CLL, some are preferentially altered in fludarabine refractoriness (FR) patients, namely TP53, NOTCH1, SF3B1 and BIRC3 [**23,25,40,42**]. FR remains an unsolved clinical problem associated with poor survival, involving 10% of patients after first-line treatment and virtually all patients after multiple lines of therapy [**43,44**]. Until recently, the molecular basis of CLL chemorefractoriness was incompletely characterized, and the only known genetic lesion with an established pathogenic role was inactivation of the TP53 gene occurring in 30% to 40% of refractory patients [**26**]. Interestingly, mutations of the splicing factor 3b, subunit 1 (SF3B1) gene have been identified in 15% of B-CLL patients [**5**] and they are recurrently associated with fludarabine-refractory CLL and poor clinical prognosis, with a frequency significantly greater than that observed in a consecutive CLL cohort sampled at diagnosis [**40**]. Therefore, SF3B1 mutated B-CLL require prompt treatment, independently of other established predictive markers [**4,45**].

In conclusion, somatic mutations affecting NOTCH1, SF3B1 and TP53 are improving our ability to predict the outcome of the disease from early stages [**41,46**], and several studies have been performed to clinically characterize the consequences of mutations affecting these genes on the prognosis of CLL. In a recent manuscript Landau et al. have shown that the presence of certain somatic mutations even in a small population of the tumor cells accurately predicts a high probability of relapse after treatment [**17**]. If this information is known at diagnosis, clinicians may choose to target those drivers early to prevent relapse [**47**].

Current management of chronic lymphocytic leukemia

The clinical course of patients with B chronic lymphocytic leukemia spans from an asymptomatic disease never requiring therapy to a rapidly progressive disorder requiring intensive treatment [**2**] The clinical heterogeneity of B-CLL and advanced age of a great number of subjects dictate that a diversified therapeutic approach, since no single treatment is applicable to all patients [**1**]. For more than 40 years, B-CLL has been treated with diverse chemotherapies [**43**]. Monotherapy with cytostatic alkylating agents, usually chlorambucil (CLB), has been used for several decades as initial, front-line therapy [**48**]; the principal limits of CLB are due to low or nonexistent complete remission (CR) rate and serious side effects after extended use, i.e. prolonged cytopenia, myelodysplasia and secondary acute leukemia [**43,48,49**]. Combinations of alkylating drugs with vinca alkaloids or anthracycline drugs did not improve outcomes [**48**]. Three purine analogs are

currently used in B-CLL, fludarabine, pentostatin, and cladribine (2-CdA). Fludarabine induced more partial remissions (PR) and more complete remissions (CR) (7%-40%) than other conventional chemotherapies, but did not improve overall survival (OS) when used as single agent [**1,50**].

A great collection of clinical data confirms that a combination of chemotherapies has proven more effective compared to monotherapy [**49**]. Since purine analogs and alkylating agents have different mechanisms of action and partially non-overlapping toxicity profiles, they were combined both in preclinical and clinical studies. The most thoroughly studied combination chemotherapy for B-CLL is fludarabine plus cyclophosphamide (FC) given as oral drugs or intravenous infusions [**51**]. Three randomized trials have demonstrated that FC chemotherapy improves clinical response, progression-free survival (PFS) and complete remission compared with fludarabine monotherapy [**52-54**]. An updated analysis of the CLL4 trial of the German CLL Study Group (GCLLSG) suggested that the front-line treatment of B-CLL patients with FC combination might improve the OS of the non-high-risk B-CLL patients [all patients without del(17p) or TP53 mutation] [**49**].

Chemo-immunotherapy was developed for the treatment of indolent and aggressive lymphoma. Rituximab, a chimeric monoclonal antibody directed against the CD20 antigen expressed on B-cells, became the standard drug for different B-cell lymphomas [**42,55**]. In B-CLL the expression of the CD20 antigen on leukemic cells is relatively low and standard-dose rituximab generates only poor response rates [**43,56**]. The results of phase 2 trials suggested that rituximab in combination with chemotherapy might have additive or synergistic effects in pretreated and treatment-naive patients [**57,58**]. In a study of 300 treatment-naïve patients, the combination of FC with rituximab resulted in an overall response rate of 95%, with 72% of patients achieving a complete response [**43,57,58**]. These response rates were among the highest reported so far for first-line treatments in patients with B-CLL [**43**]. Furthermore, this clinical study documented that patients with del(11q) presented complete remission after chemo-immunotherapy and patients with trisomy 12 and del(13q) greatly benefited from treatment. On the contrary, patients with del(17p), associated with a dysfunction of the p53 tumour suppressor and a very poor outcome, might not benefit substantially [**43**].

Immunotherapies for B-CLL treatment include other two drugs, which demonstrate therapeutic efficacy. Ofatumumab is a fully humanized antibody targeting the CD20 antigen, that induces an increased cell death due to greater complement-dependent cytotoxicity and similar antibody-dependent cellular-cytotoxicity activity compared with rituximab. Ofatumumab has shown some efficacy in patients with fludarabine and alemtuzumab refractory or bulky disease [**59**]. Alemtuzumab is a recombinant, fully humanized monoclonal antibody against the CD52 antigen.

Monotherapy with alemtuzumab had high response rates in patients with advanced B-CLL previously treated with alkylating agents and in patients nonresponsive or relapsed after second-line fludarabine therapy [**49**]. In addition, alemtuzumab has proven effective in patients with high-risk genetic markers such as deletions of chromosome 11 or 17 and TP53 mutations [**60**].

Currently numerous new compounds that target a relatively specific signaling defect or redirect the immune system against B-CLL cells are in clinical development [**61,62**]. These agents show clinical efficacy and may yield response rates above 50% even in relapsed and refractory CLL patients [**43**]. In particular, agents targeting B cell receptor (BCR) signaling have entered in phase 3 trials for B-CLL patients. Stimulation of BCR induces the activation of different tyrosine kinases, such as Bruton tyrosine kinase (BTK), spleen tyrosine kinase (Syk), ZAP-70, Src family kinases, and phosphatidyl inositol 3-kinase (PI3K), which stimulate malignant B-cell survival via activation of transcription factors such as NF-kB [**61,63**]. Idelalisib (CAL-101), an oral PI3Kp100δ isoform–selective inhibitor, promotes apoptosis selectively in primary B-CLL cells, without reducing antibody-dependent cellular cytotoxicity [**64**]. In a phase 1 clinical trial in 54 heavily pretreated and high-risk B-CLL patients, idelalisib showed acceptable toxicity, positive pharmacodynamics effects, and favorable clinical activity. An overall response rate (ORR) of 56% was achieved, with 2 CRs and 28 PRs [**65**].

Ibrutinib (PCI-32765) is an orally active small molecule inhibiting BTK, which activates cell survival pathways such as NF-kB and MAPKs via Src family kinases. Inhibition of BTK might induce apoptosis in B-cell lymphomas and B-CLL cells [**66**]. Ibrutinib showed significant activity in patients with relapsed or refractory B-CLL [**67**]. Data from a phase 1b-2 multicenter study with single-agent ibrutinib on 85 patients with relapsed or refractory B-CLL or small lymphocytic lymphoma, the majority with high-risk disorder, were published recently [**68**]. The ORR was 71%, the majority being PRs (68%). Interestingly, the response was independent of clinical and genomic risk factors, including advanced stage disease, the number of previous therapies and del(17p). This study illustrates that ibrutinib may soon become an additional treatment option for B-CLL patients with high-risk genetic lesions [**68**]. The above described novel therapies, targeting specific signaling proteins of B-CLL cells, present a moderate overall toxicity, without myelosuppression. However, CRs have not occurred frequently so far with any of these newer agents [**43**].

Patients who relapse and have not acquired a TP53 abnormality can be expected to respond to a further course of their initial therapy, although the PFS is usually shorter than after initial therapy and repeated courses often lead to drug resistance. However, re-treatment with the previous therapy is not recommended in patients whose initial treatment was sub-optimal or if a new treatment, shown

to be superior to the initial therapy, becomes available [**1**]. For patients with high risk B-CLL (TP53 defect and/or failing fludarabine combination therapy within 2 years), results of phase II and III studies using either FC, FCR or alemtuzumab, with or without high dose steroids, indicate that alemtuzumab plus pulsed methylprednisolone or dexamethasone should be regarded as the induction regimen of choice. However, this regimen is associated with a significant risk of infection and the duration of remission is relatively short. Allogeneic stem-cell transplantation provides the last opportunity of achieving long-term disease-free survival for patients with high-risk B-CLL, particularly those with TP53 defects [**1,43**].

Metabolic transformation in cancer

Over the past 25 years, the oncogene revolution has stimulated the research in cancer biology, revealing that the crucial phenotypes of tumour cells result from a host of mutational events that combine to alter multiple core signaling pathways [**69,70**]. High-throughput sequencing data suggest that the mutations leading to tumorigenesis are even more numerous and heterogeneous than previously thought [**71**]. Indeed, gene set enrichment analysis showed significant up-regulation of several core processes, known to participate also in cancer metabolic reprogramming, such as glycolysis/gluconeogenesis, the pentose phosphate pathway or oxidative phosphorylation [**72,73**]. Multiple key oncogenic signalling pathways converge to adapt tumour cell metabolism in order to support their growth and survival. Some of these metabolic alterations, that is rapid ATP generation, increased biosynthesis of macromolecules and tightened maintenance of cellular redox status, seem to be absolutely required for malignant transformation. Therefore, altered cellular metabolism represents one of the emerging hallmark of cancer [**69,73,74**].

The most evident and most studied metabolic phenotype observed in tumour cells is the Warburg effect, also termed aerobic glycolysis, which describes the shift from ATP generation through oxidative phosphorylation to ATP generation through glycolysis [**75**]. Indeed while normal tissues used mitochondrial oxidation to account for 90% of ATP production with glycolysis accounting for 10%, tumor cells used less of the highly efficient oxidative phosphorylation, producing 50% of the ATP from oxidation and 50% from glycolysis. This shift was thought to occur even though there is sufficient oxygen to support mitochondrial function [**76,77**]. The increase in glycolysis at the expense of mitochondrial energy production helps to support unbridled growth, provide precursors for the biosynthesis of macromolecules and protect cells from excessive and toxic levels of reactive

oxygen species (ROS) and oxidative stress [**69**]. This hypothesis greatly influenced the present perception of cancer metabolism, moving aerobic glycolysis into the mainstream of clinical oncology.

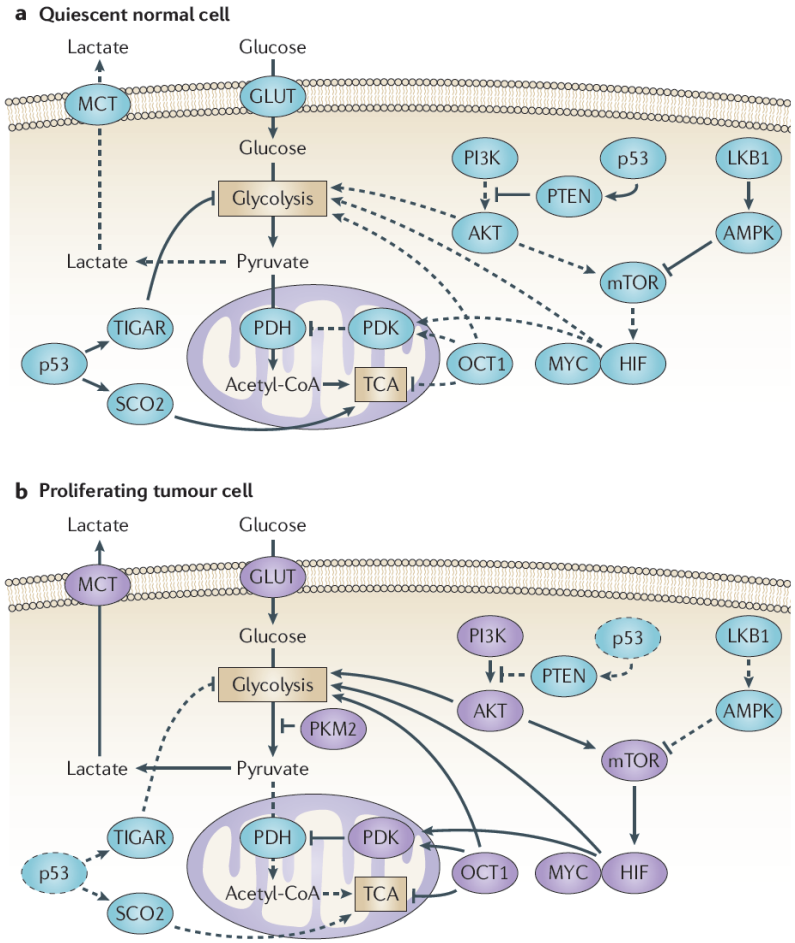

Figure 1. Molecular mechanisms driving the Warburg effect. Relative to normal cells (part a) the shift to aerobic glycolysis in tumour cells (part b) is driven by multiple oncogenic signalling pathways. PI3K activates AKT, which stimulates glycolysis by directly regulating glycolytic enzymes and by activating mTOR. The liver kinase B1 (LKB1) tumour suppressor, through AMP-activated protein kinase (AMPK) activation, opposes the glycolytic phenotype by inhibiting mTOR. mTOR induces the glycolytic phenotype by enhancing hypoxia-inducible factor 1 (HIF1) activity, which engages a hypoxia-adaptive transcriptional programme. HIF1 increases the expression of glucose transporters (GLUT), glycolytic enzymes and pyruvate dehydrogenase kinase, isozyme 1 (PDK1), which blocks the entry of pyruvate into the tricarboxylic acid (TCA) cycle. MYC cooperates with HIF in activating several genes that encode glycolytic proteins, but also increases mitochondrial metabolism. The tumour suppressor p53 opposes the glycolytic phenotype by suppressing glycolysis through TP53-induced glycolysis and apoptosis regulator (TIGAR), increasing mitochondrial metabolism via SCO2 and supporting expression of PTEN. OCT1 acts in an opposing manner to activate the transcription of genes that drive glycolysis and suppress oxidative phosphorylation. The switch to the pyruvate kinase M2 (PKM2) isoform affects glycolysis by slowing the pyruvate kinase reaction and diverting substrates into alternative biosynthetic and reduced nicotinamide adenine

dinucleotide phosphate. (NADPH)-generating pathways. MCT, monocarboxylate transporter; PDH, pyruvate dehydrogenase. The dashed lines indicate loss of p53 function. *Image from Cairns et al,2011.*

Recent advances in genomics and proteomics have provided insights into molecular mechanisms which underline the metabolic remodelling occurring in cancer cells [**73,75**]. Metabolic pathways in normal cells are tightly regulated and all parts of these networks can be highly perturbed in cancer cells [**78**]. Mutations in oncogenes and tumour suppressor genes cause alterations to multiple intracellular signaling pathways that affect tumour cell metabolism and reengineer it to allow enhanced survival and growth [**69,71**]. Consistently genetic analysis of tumors has since identified numerous oncogenes that, once activated, increase glycolysis and glutaminolysis, and, analogously, different tumor suppressor that, once lost, can shift energy production away from the mitochondria to a more glycolytic equilibrium [**75,79**]. Irrespective of the mechanisms involved, if certain tumors are reliant on glycolysis for bioenergetics, biosynthesis and invasive potential, therapeutic targeting of the underlying pathways may result in an anti-tumor activity (Figure 1) [**79,80**]. Indeed drugs that can selectively target the metabolic phenotype of the tumour are likely to at least delay tumour progression [**74**]. The resistance of tumours to both radiotherapy and chemotherapy can often be attributed to its aberrant metabolism. Therefore the reactivation of a more 'normal' metabolism could re-sensitize tumours to these agents. From a therapeutic perspective, knowledge of cancer cell metabolism will enable the identification of new drug targets and will facilitate the design of a new class of cancer therapeutics and diagnostic tools especially exciting [**69**]. The ultimate aim is to develop treatment strategies that slow tumour progression, improve the response to therapy and result in a positive clinical outcome [**81**]. Therapies that target tumour metabolism are currently being tested in pre-clinical and clinical studies [**74**].

Metabolism in chronic lymphocytic leukemia

Despite the high incidence of B chronic lymphocytic leukemia, metabolism of B-CLL cells remains a relatively unexplored field [**82**]. Although initially demonstrated in solid tumors, a recent study identified dysregulated glucose metabolism as a novel therapeutic target also in B-CLL [**83**]. In particular glycolytic enzymes appeared to be upregulated in a subset of CLL patients with either higher white blood cell counts and/or more aggressive clinical course. Additionally recent evidences documented that in leukemic cells mitochondrial uncoupling, i.e. the reduction in ATP synthesis in response to mitochondrial membrane potential, due to the overexpression of uncoupling protein UCP2, promotes glycolysis, increases the apoptotic threshold and induces chemo-resistance [**84**].

Results from few studies indicate that B-CLL cells might contribute to the so-called cancer-associated oxidative stress [**85**]. This metabolic condition results from accumulating reactive oxygen species (ROS) [**86**], compared with normal B-cell, due to cancer-related mitochondrial alterations, such as defective oxidative phosphorylation or an enhanced mitochondrial biogenesis [**87**]. Moreover, high levels of ROS correlated with the number of circulating CLL cells and have been detected in more aggressive B-CLL cells [**88**]. Mitochondria were identified as the key source for abundant ROS in B-CLL [**76**,**82**]. Escalated ROS levels promote genetic instability and development of drug resistance, determine alterations in cell-signaling [**86**] and altogether account for cancer cells' aggressive behavior [**82**]. This is in line with studies demonstrating that B-cell stimulation promotes ROS production [**89**] and B-CLL cells partially resemble chronically activated B-cells [**90**]. Oxidative stress additionally attenuates immune responses by leading to dysfunctions and even apoptosis of NK- and T-cells, suggesting a role in tumor immune-escape [**82**]. Since cancer cells are continuously exposed to high levels of endogenous ROS, cells which adapt to high stress condition are preferentially selected. Consequently, an enhanced protective antioxidant capacity is reported in tumors, which in addition induce the development of drug resistance [**91**]. As a protective measure, the activation of the redox adaptive cascade (through increased expression of intracellular antioxidant catalase and the stress-responsive heme oxygenase-1, and reduced expression of mitochondrial manganese superoxide dismutase) would then additionally promote biogenesis of novel and functional mitochondria [**82**]. Thus increased mitochondrial ROS, adaptation to intrinsic oxidative stress and mitochondrial biogenesis are interconnected in B-CLL.

Interestingly, using agents that further aggravate mitochondrial ROS production and thereby overwhelm the cancer cells' protective systems could selectively induce apoptosis in B-CLL cells [**82**]. Metabolic alterations can render malignant cells more susceptible to perturbations and therefore agents directed against the unique metabolic features of B-CLL cells might represent an opportunity to improve current therapeutic treatments and even to overcome drug resistance within B-CLL cells.

Targeting aerobic glycolysis in chronic lymphocytic leukemia

Several recent studies have confirmed that restricting glycolysis or diverting pyruvate into the mitochondria can significantly induce respiration in cancer cells [**92**]. The fate of pyruvate [either reduction in the cytosol by lactate dehydrogenase (LDH) or oxidation in the mitochondria by pyruvate dehydrogenase (PDH)] determines the direction of tumour metabolism. The inhibition of lactate dehydrogenase or the activation of pyruvate dehydrogenase can induce tumour cells to oxidize pyruvate in the TCA cycle and stimulate mitochondrial respiration [**93-95**]. Pyruvate dehydrogenase

represents the enzymatic step linking glycolysis to oxidative phosphorylation. One of four pyruvate dehydrogenase kinase (PDKs) and one of two pyruvate dehydrogenase phosphatases are associated with PDH and regulate the phosphorylation of the E1a subunit, dictating PDH activity. When phosphorylated, PDH is inactivated, resulting in channelling of pyruvate to lactate, whereas the non-phosphorylated form is active and converts pyruvate into mitochondrial acetyl-CoA [**5**]. Recent studies provided evidence that PDK1 expression is elevated in cancers, thereby attenuating mitochondrial function and respiration, and its activation may be a key regulatory switch contributing to the Warburg effect [**5**,**69,70,77**]. The inhibition of PDK is increasingly becoming seen as a valid target for cancer therapy [**14,81**]. Indeed ihibitors of PDK could potentially reverse some of the metabolic effects of tumorigenic signalling and several such candidates, including the mitochondria-targeting dichloroacetate molecule (DCA), are currently under evaluation for their therapeutic utility [**71,74,75**]. Indeed, preclinical studies confirm the relatively low toxicity of DCA and document its efficacy against numerous epithelial cancers (such as non-small cell lung, endometrial, prostate, breast and colorectal cancer), glioblastoma, as well as multiple myeloma [**96-105**]. DCA inhibits mitochondrial pyruvate dehydrogenase kinase (PDK) reverting the metabolic-electrical remodelling occurring in cancer cells; indeed it shifts the metabolism from glycolysis to glucose oxidation. In addition, DCA decreases the mitochondrial membrane potential, increases the reactive oxygen species (ROS) production and ultimately induces apoptosis and tumor growth arrest in mice models, without apparent toxicity [**95**]. DCA is an orally bioavailable, small molecule and currently being evaluated in phase I/II clinical trials for glioblastoma, gliomas and other solid tumors [**106**]. Interestingly, in solid tumor models it has also been reported that DCA may activate p53 [**107**]. In addition, a couple of recent studies proposed DCA alone or in association with bortezomib for the treatment of multiple myelomas [**105,108**], suggesting anti-cancer activity of DCA also in hematological disorders.

The oncosuppressor TP53: role in metabolic transformation

Although the tumour suppressor p53 is best known for its functions in mediating the cytotoxic response of most therapeutic molecules currently used in cancer therapy, p53 is also an important regulator of metabolism [**69**]. The role of p53 as a central component of the stress response machinery is well established, and numerous forms of stress - many of which are encountered during tumoral transformation - lead to the activation of p53 [**109**]. Virtually any stress signal can induce

p53, including hypoxia or the lack of nutrients and deregulated signalling through the nutrient-sensing pathways, namely the AKT–mTOR pathway [**110**]. Oxidative stress regulates p53 function by directly affecting its redox state and oxidation [**111**] and mitochondrial ROS represent an important component of the stress-induced activation of p53 [**112**]. Also, p53 is efficiently activated by ribosomal stress through the ability of several ribosomal proteins to bind and inactivate MDM2 [**113**]. Combinations of these abnormalities during tumour progression amplify the protective p53 response. However, increased glucose metabolism stimulated by the expression of the glucose transporter GLUT1 or hexokinase has been reported to suppress p53 activity [**114**], suggesting that high levels of glycolysis in cancer may help evade the tumour-suppressive effects of p53. The most obvious advantage of p53 activation under conditions of metabolic stress is a coordinated inhibition of cell proliferation and growth. However additional consequences of p53 activation are being uncovered, including an ability of p53 to promote the use of certain metabolic pathways and to increase cell survival.

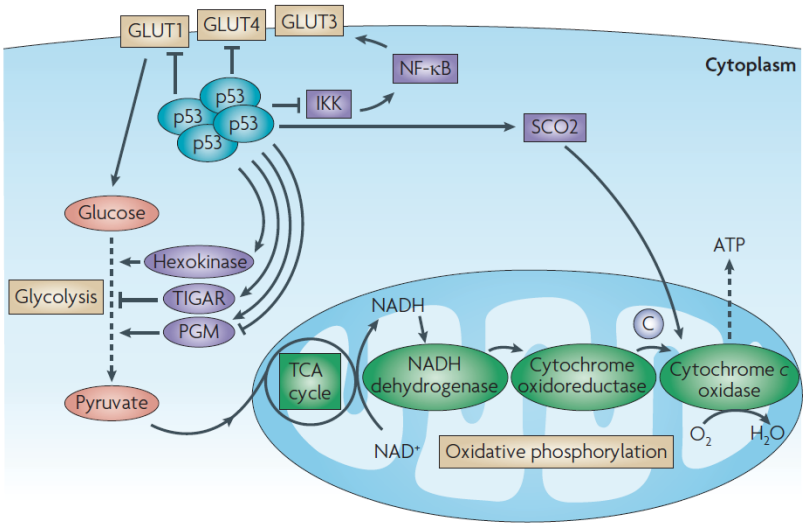

Figure 2. Regulation of energy production by p53. Several functions of p53 reduce the flux through the glycolytic pathway and increase oxidative phosphorylation, thereby opposing the Warburg effect, in which cancer cells predominantly use glycolysis for energy production. However, there are also activities of p53, such as the activation of hexokinase and phosphoglycerate mutase (PGM), which could increase glycolysis under some circumstances. GLUT, glucose transporter; IKK, IκB kinase; NF-κB, nuclear factor-κB; SCO2, synthesis of cytochrome c oxidase 2; TCA, tricarboxylic acid. *Image from Vousden and Ryan,2009.*

Several studies documented that p53 exerts a role in the regulation of both glycolysis and oxidative phosphorylation (Figure 2) [**78**]. Different mechanisms have been described through which

p53 can slow glycolysis and therefore counteract its increase in cancer. p53 can inhibit the expression of the glucose transporters GLUT1 and GLUT4 and can decrease the levels of phosphoglycerate mutase (PGM), while increasing the expression of TP53-induced glycolysis and apoptosis regulator (TIGAR), which reduces the levels of the glycolytic activator fructose-2,6-bisphosphate [**78,115**]. Wild-type p53 also supports the expression of PTEN, which inhibits the PI3K pathway, thereby suppressing glycolysis [**116**] and hexokinase 2 (HK2), which converts glucose to glucose-6-phosphate (G6P) [**117**]. G6P then either enters glycolysis to produce ATP, or enters the pentose phosphate pathway. The effect of each of these actions is to impede flux through different steps of the glycolytic pathway. The restraint on glycolytic rate imposed by p53 is in accordance with its ability to help maintain mitochondria and drive oxidative phosphorylation [**118**]. These effects are the consequence of several p53-dependent functions, including the transcriptional activation of subunit I of cytochrome *c* oxidase [**119**]; the activation of expression of synthesis of cytochrome *c* oxidase 2 (SCO2), a key regulator which is required for the assembly of the cytochrome *c* oxidase complex of the electron transport chain [**120**]; and the induction of expression of the ribonucleotide reductase subunit p53R2 protein, that contributes to the maintenance of mitochondrial DNA [**121**]. Loss of either p53 or SCO2 expression results in a switch from cellular respiration to aerobic glycolysis, suggesting that inactivation of p53 in human cancers may directly contribute to the Warburg effect [**75,122**]. Indeed in tumors with non-functional p53 (majority of tumors), the mitochondrial electron-transport chain is compromised, and glycolysis is the more efficient mechanism for generation of ATP [**80**]. Interestingly, several of these p53 activities, such as the regulation of SCO2, seem to function under normal growth conditions in the absence of an acute stress signal, suggesting that p53 can help to maintain the aerobic respiration of most normal cells. However, the presence of p53-responsive elements in the promoters of phosphoglycerate mutase and hexokinase II suggests that p53 can promote at least some steps in glycolysis, resulting in increased survival signalling by helping to limit ROS production [**78**]. These different activities reflect context- or tissue-dependent differences in the metabolic functions of p53. Notwithstanding the role of p53 in enhancing oxidative phosphorylation, increased glycolysis in response to pharmacological inhibition of oxidative phosphorylation is reported to be dependent on p53 [**123**].

Our recent appreciation of the importance of basal levels of p53 in regulating metabolic pathways is mirrored by the importance of the antioxidant functions of low or uninduced levels of p53 [**124**]. ROS are heterogeneous in their properties and exert a plethora of downstream effects, depending on the concentrations at which they are present. Low levels of ROS are required for homeostatic signaling events, increasing cell proliferation and survival through the post-translational

modification of kinases and phosphatases [**125**]. At moderate levels, ROS induce the expression of stress-responsive genes such as hypoxia-inducible factor HIF-1A, which in turn determine the expression of proteins providing pro-survival signals [**69**]. However, once levels of ROS become excessively high, they cause damage to macromolecules, induce the activation of protein kinase Cδ (PKCδ) and senescence [**126**], and/or cause permeabilization of the mitochondria, with the release of cytochrome *c* and apoptosis [**127**]. Cells counteract these effects of ROS by producing antioxidant molecules, such as reduced glutathione and thioredoxin [**69**]. There is currently a scientific consensus that cancer cells alter their metabolic pathways and regulatory mechanisms so that ROS and antioxidants are tightly controlled and maintained at higher levels than in normal cells, in such a way that the cell survives and the levels of ROS are reduced to moderate levels [**128,129**]. The mechanisms designed to counter the control of ROS abundance allow the cancer cell to avoid the detrimental effects of high levels of ROS, but also increase the chance that cell will experience additional ROS-mediated mutagenic events and stress responses that promote tumorigenesis.

p53 may promote oxidative stress while inducing apoptosis, but it also exerts an important role in reducing oxidative stress as a defense mechanism. Interestingly, through the p53 target gene cyclin-dependent kinase inhibitor 1A (CDKN1A, which encodes p21), p53 promotes the stabilization of the transcription factor NRF2 [**130**]. NRF2 is the master antioxidant transcription factor and upregulates the expression of several antioxidant and detoxifying molecules [**130**]. Loss of p53 in a cancer cell inactivates this redox maintenance mechanism: because p21 is not activated, NRF2 continues to be degraded, antioxidant proteins are not expressed and the redox balance is lost [**130**]. Regulation of the glycolytic pathway by p53 can also help to modulate oxidative stress by increasing flux through the pentose phosphate pathway. The activation of both TIGAR and hexose-6-phosphate dehydrogenase would promote the pentose phosphate pathway, with the generation of NADPH that enters in both anabolic and antioxidant pathways [**78**].

p53 can also exerts strong pro-oxidative effects. The ability of p53 to induce senescence and apoptosis is clearly related to the induction of oxidative stress, and even necrotic cell death is activated by the cooperation between ROS and p53-induced cathepsin Q expression [**78**]. Several p53-inducible proteins activated during the apoptotic response promote ROS production, including p53-induced gene 3 (PIG3), proline oxidase, Bax, PUMA and p66Shc [**78**]. To further increase this effect, p53 can also inhibit or modulate the expression of antioxidant genes such as superoxide dismutase 2 (SOD2), aldehyde dehydrogenase 4 (ALDH4) and glutathione peroxidase 1 (GPx1), which increases oxidative stress [**78**]. Less directly, the ability of p53 to drive oxidative phosphorylation through the activation of SCO2 will also promote the generation of ROS from the

mitochondria [**120-122**]. Depending on the cell type and the levels of ROS, the consequences of ROS regulation by p53 can include proliferation, migration, genotoxic damage, senescence and cell death. In cells in which both pro-oxidant and antioxidant responses are possible the difference lies in the extent and persistence of the damage-inducing stress. The regulation of ROS by p53 might be different under basal or low-stress conditions (in which p53 functions as an antioxidant) compared with high-damage and high-stress conditions (in which p53 contributes to cell death by increasing ROS levels) [**131**]. From a clinical point of view, it may be possible to exploit loss-of-function p53 mutations or other tumour suppressor genes by applying additional oxidative stress. In the absence of the redox maintenance pathway that is supported by these tumour suppressors, malignant cells might be selectively killed [**86**].

Numerous data indicate a role of wild-type p53 in averting metabolic transformation, although the possible role of mutant p53 is as yet largely unexplored. TP53 incurs point mutations in numerous cancers, with expression of mutant p53 proteins that have acquired activities which contribute to malignant progression independently of the loss of wild-type p53 function. A role for these mutant p53 proteins in promoting the metabolic transformation would be extremely interesting.

Targeting p53 with Nutlin-3 as potential therapeutic option for B-CLL

The cellular level of the protein p53 is regulated primarily by degradation via the ubiquitin-proteasome pathway, and the murine double minute 2 gene (MDM2) functions as a master regulator of p53 [**132**]. Vassilev et al. [**133**] reported the first potent and selective small molecule antagonist of MDM2, termed Nutlin-3. This is a *cis*-imidazoline analogue that binds to the p53 pocket on the surface of MDM2, activating the p53-pathway *in vitro* and *in vivo*. Notably, this interaction, while blocking MDM2-mediated inhibition of p53, does not interfere with p53 function and has little toxicity in animal models. In this context, Secchiero et al. demonstrated that Nutlin-3 is effective in inducing apoptosis *in vitro* in $p53^{wild\text{-}type}$ B-CLL samples independently of the negative prognostic markers [**134-136**], as confirmed by other authors. These studies strengthened the concept that selective, non-genotoxic activation of p53 might represent an alternative to the current cytotoxic chemotherapy.

Interestingly, Nutlins not only induced apoptotic death in leukemic cells, but also showed a synergistic effect when used in combination with the chemotherapeutic drugs commonly used for the treatment of hematological disorders. Furthermore Nutlins also exert non cell-autonomous biological activities, such as inhibition of vascular endothelial growth factor, stromal derived factor 1/CXCL12 and osteoprotegerin expression and/or release by primary fibroblast and endothelial cells. Moreover, Nutlins have a direct anti-angiogenetic and anti-osteoclastic activities. Thus Nutlins might have

therapeutic effects by two distinct mechanisms: a direct cytotoxic effect on leukemic cells and an indirect non-cell autonomous effect on tumor stromal and vascular cells, and this latter effect might be therapeutically relevant also for treatment of leukemia with 53 mutations [**129**]. Furthermore, it is noteworthy that, when used in association with other therapeutic compounds, Nutlin-3 showed synergistic cytotoxic activity also on $p53^{mutated}$ B-CLL cells [**136,137**].

Objectives

In spite of the recent therapeutic advances in the treatment of B-CLL patients, a major unsolved clinical problem is represented by the lack of effective treatments for B-CLL patients with more aggressive disease, carrying cytogenetic abnormalities affecting the p53-pathway activation (17p13.1 or 11q22.3 deletions), or characterized by recently identified somatic mutations in TP53, NOTCH1, SF3B1 and BIRC3 genes, who are less likely to respond to conventional treatments. Additionally, recurrent and/or relapsing disease remains a major concern. Taken together, these data underline the need to investigate new compounds for innovative anti-leukemic targeted therapies with less toxicity and increased efficacy, to be used alone or in combination with other therapeutics.

On these bases, the broad objective of my project was to preclinically assess the effects of the glycolytic inhibitor DCA in B-CLL *in vitro*. Particular attention has been directed to assess the potential therapeutic efficacy towards the B-CLL subtypes characterized by poor prognosis (i.e. p53 mutations). In order to achieve this aim, the experimental plan was structured in two phases:

i) we assessed the cytotoxic/cytostatic effects of DCA in a collection of primary $p53^{wild\text{-}type}$ B-CLL samples obtained from patients and in normal peripheral blood mononuclear cells (PBMC), as well as a panel of human $p53^{wild\text{-}type}$ B leukemic cell lines (EHEB, JVM-2, JVM-3). DCA was used either alone and in association with Nutlin-3. In addition, we have investigated the key intracellular molecular determinants mediating the activity of DCA, Nutlin-3 and Nutlin-3+DCA;

ii) we evaluated the cytotoxic/cytostatic effect of DCA in primary $p53^{mutated}$ B-CLL cells and in human $p53^{mutated/null}$ leukemic cell lines (MAVER, MEC-1, MEC-2, HL-60). In order to dissect the p53-independent molecular mechanisms of DCA cytotoxicity, a set of experiments based on proteomic and genomic approaches was performed using the $p53^{null}$ HL-60 leukemic cell line.

Methods

Primary B-CLL patient samples and B leukemic cell lines

For experiments with primary cells, peripheral blood samples were collected in heparin-coated tubes from B-CLL patients and healthy blood donors following informed consent, in accordance with the Declaration of Helsinki and in agreement with institutional guidelines (University-Hospital of Ferrara). The main clinical parameters of the B-CLL patients were abstracted from clinical records (Table 2). All patients had been without prior therapy at least for three weeks before blood collection. Peripheral blood mononuclear cells (PBMC) were isolated by gradient centrifugation with lymphocyte cell separation medium (Cedarlane Laboratories, Hornby, ON, CAN). T lymphocytes, NK lymphocytes, granulocytes and monocytes were negatively depleted from peripheral blood B-CLL with immunomagnetic microbeads (MACS microbeads, Miltenyi Biotech, Auburn, CA), with a purity >95% of resulting CD19+ population, as assessed by flow cytometry analysis.

To analyze the TP53 status, selected B-CLL patients' DNA samples obtained from circulating $CD19^+$ cells were sequenced on Ion Torrent Personal Genome Machine system using a custom Ion AmpliSeq panel (Life Technologies, Carlsbad, CA) targeting the exonic regions and the exon-intron boundaries of TP53. Next generation sequencing data was annotated by a standard ANNOVAR pipeline supplied by COSMIC v68 database. All selected variants were validated by Sanger sequencing, first on genomic DNA and in case of splicing variants on cDNA. The potential pathogenicity of the identified mutations and their effects on p53 functionality was predicted by web tools (SIFT, http://sift.jcvi.org/; PolyPhen-2, http://genetics.bwh.harvard.edu/pph2/; MutationTaster, http://www.mutationtaster.org/; HSF, http://www.umd.be/HSF; NNSplice, http://www.fruitfly.org/seq_tools/splice.html) and by protein structural bioinformatics analysis (NCBI, http://www.ncbi.nlm.nih.gov/protein/; PDB, http://pdb.org; UniProt, http://www.uniprot.org; PFAM, http://pfam.sanger.ac.uk). The main clinical and molecular parameters of the selected B-CLL patients are reported in Table 4.

For the *in vitro* assays, B-CLL patients' cells were cultured in RPMI-1640 medium containing 10% FBS, L-glutamine and Penicillin/streptomycin (all from Gibco, Grand Island, NY) and used

within the first 48 hours of cultures. The $p53^{wild\text{-}type}$ B leukemic cell lines EHEB, JVM- 2, JVM-3, the $p53^{mutated}$ B lymphoblastoid leukemic cell lines MAVER, MEC-1 and MEC-2 and the $p53^{null}$ HL-60 leukemic cell line were all purchased from DSMZ (Deutsche Sammlung von Mikroorganismen und Zellkulturen GmbH, Braunschweig, Germany). The $p53^{wild\text{-}type}$ B leukemic cell lines, MAVER and HL-60 cell lines were routinely cultured in RPMI-1640, whereas MEC-1 and MEC-2 were maintained in IMDM, all supplemented with 10% FBS, L-glutamine and Penicillin/streptomycin (all from Gibco).

Culture treatments, assessment of cell viability, apoptosis, cell cycle profile and senescence

For *in vitro* treatments with DCA (Sigma-Aldrich, St Louis, MO), used either alone or in combination with Nutlin-3 (Cayman Chemicals, Ann Arbor, MI), cells were seeded at a density of $1x10^6$ cells/ml and cultured under normoxic conditions. At different time points after treatment, cell viability was examined by Trypan blue dye exclusion and MTT (3-(4,5-dimethilthiazol- 2yl)-2,5-diphenyl tetrazolium bromide) colorimetric assay (Roche Diagnostics Corporation, Indianapolis, IN) for data confirmation. Levels of apoptosis were quantified by Annexin V-FITC/ propidium iodide (PI) staining (Immunotech, Marseille, France) followed by analysis using a FACSCalibur flow cytometer (Becton-Dickinson, San Jose, CA). To avoid non-specific fluorescence from dead cells, live cells were gated tightly using forward and side scatter. The cell cycle profile was analyzed by flow cytometry after 5-bromodeoxyuridine (BrdU) incorporation. Briefly, leukemic cells were incubated with 50 μM BrdU (Sigma-Aldrich) at 37°C for 1 hour. The antibody anti-BrdU (BD Biosciences Pharmingen, San Diego, CA) was bound to BrdU incorporated into neosynthesized DNA and the complex was detected by FITC conjugated secondary antibody (Immunotech). Cells were then stained with PI (50 μg/mL) and analyzed by flow cytometry. Senescence was assessed under light microscope by senescence-associated β-galactosidase (SA-β-gal) staining, using a specific kit (Abcam, Cambridge, UK) and following the manufacturer's instructions.

Assessment of mitochondrial alterations

Mitochondrial activity was evaluated staining cells with MitoTracker® GreenFM (Molecular Probes, Inc., Eugene, Oregon), which passively diffuses across the plasma membrane and accumulates in active mitochondria. Briefly, at different time points, cells were incubated with pre-warmed MitoTracker staining solution (obtained diluting MitoTracker® GreenFM in serum-free medium to a final concentration of 25 nM) for 30 minutes at 37°C. Cells were then washed with PBS (Gibco) and analyzed by flow cytometry.

The presence of morphological signs characteristic of mitochondrial alteration, such as mitochondrial fragmentation and cristae remodeling, were analyzed by transmission electron microscopy. Mitochondrial activity was evaluated by measuring the cellular ATP production. Briefly, ATP concentration was determined using the ATP Assay KIT (Abcam) in cell lysates of untreated and DCA treated cultures at different time points. Measurements were performed with the colorimetric method, following the manufacturer's instructions. ATP contents were normalized per number of cells.

Western blot analyses

For Western blot analysis, cells were lysed and protein determination was performed by using the BCA Protein Assay (Thermo Scientific, Rockford, IL). Samples were supplemented with loading buffer (250 mM Tris pH 6.8, 2% SDS, 10% glycerin, 4% beta-mercaptoethanol, 1% bromophenol blue) and boiled for 2 minutes. Equal amounts of protein for each sample were migrated in SDS-polyacrylamide gels and blotted onto nitrocellulose filters. The following Abs were used: anti-p53 (DO-1), anti-MDM2 (SMP14), anti-p21 (C-19), anti- PUMAα/β (H-136), anti-PARP-1 (H-250) and anti- Bax (2D2) purchased from Santa Cruz Biotechnology (Santa Cruz, CA); anti-Phospho-p53 (Ser15) and anti- Phospho-p53 (Ser392) from Cell Signaling Technology (Danvers, MA); anti-tubulin from Sigma-Aldrich. After incubation with anti-mouse or anti-rabbit IgG horseradish peroxidase-conjugated secondary Abs (Sigma-Aldrich), specific reactions were revealed with the ECL Lightning detection kit (Perkin Elmer, Waltham, MA). Densitometry values for Western blot were estimated by the ImageQuant TL software (GE Healthcare, Buckinghamshire, UK) and were expressed as arbitrary units (a.u.). Multiple film exposures were used to verify the linearity of the samples analyzed and to avoid saturation of the film.

Bi-dimensional gel electrophoresis (2-DE) and immunoblotting

For bi-dimensional gel electrophoresis, protein extraction was performed by adding 150 µl of lysis buffer (5M urea, 2M tiourea, 2% CHAPS, 2% Zwittergent detergent; all from Calbiochem, San Diego, CA) with protease inhibitors (Complete, mini EDTA-free mixture, Roche Applied Science, Milan, Italy) to the cell pellets. Lysates were sonicated for 3 min, and 250 units of benzonase endonuclease (Novagen, San Diego, CA) were added to each sample and incubated for 40 minutes at room temperature on rotary shaker. Cell debris were removed by centrifugation at 13000 x g for 10 minutes, 15°C. The supernatants were aliquoted and stored at −80°C. Protein concentration was measured with a modified Bradford method (BioRad, Milan, Italy). Protein extracts (30 µg) from each

sample were diluted to a final volume of 125 µl in the rehydration solution (5M urea, 2M thiourea, 2% CHAPS, 2% Zwittergent, 100 mM DeStreak, 0.5% IPG buffer pH 3–10 linear; all from GE Healthcare) and then applied on immobilized pH 3–10 linear gradient strips, 7 cm (IPG strips, GE Healthcare). Briefly, IPG strips were hydrated on an IPGphor apparatus (GE Healthcare) for 16 h at 30 V/h and then focused for 26 h until 50,000 V-h. After the first-dimension run, proteins were reduced by LDS Sample Buffer (Life Technologies, Carlsbad, CA) containing 60 mM DTT (GE Healthcare). Proteins were alkylated by 100 mM iodoacetamide (Sigma-Aldrich). The strips were then embedded in 0.7% (w/v) agarose on the top of 1-mm-thick acrylamide precast gels at 10% (Life Technologies). After electrophoresis the proteins were transferred to nitrocellulose membrane by standard electroblotting and stained with MemCode™ Reversible protein stain kit (Fisher Scientific, Illkirch Cedex, France). After blocking with 5% dry milk in TBS-Tween20 for 1 h at room temperature, the membranes were probed with an anti-p53 (DO-1) antibody (Santa Cruz Biotechnology) and then exposed to the peroxidase-linked specie specific anti-mouse IgG (Sigma-Aldrich). The p53 positive proteins were visualized using chemiluminescence plus (ECL plus) Western blotting detection reagents (GE Healtcare).

Proteomic profiling

To perform one-dimensional gel electrophoresis (1-DE), for each experimental group triplicates of HL-60 cell protein extract (25 µg/replicate) were mixed with equal volume of Laemmli sample buffer and resolved on a NuPAGE® Novex® 4-12% Bis-Tris gel (Life Technologies). Each gel lane was manually cut with a sterile surgical blade into 24 bands of equal height (about 3 mm) and excised bands were crushed into small fragments, processed, submitted to in-gel trypsin digestion and peptide extractions. An aliquot of each digest (2 µl) was directly analyzed by liquid chromatography-tandem mass spectrometry (LC-MS/MS) using a LTQ Orbitrap XL™ (Thermo Scientific), interfaced with a 1200 series capillary pump (Agilent Technologies Inc., Santa Clara, CA).

For protein identification, tandem mass spectra were extracted and the charge states deconvoluted by BioWorks version 3.3.1 (Thermo Scientific). For each sample, the MS/MS data from the 24 gel bands were merged and submitted as “mgf” file to the search engine Mascot (in-house version 2.2.06, Matrix Science, London, UK). Scaffold (version 3_00_02, Proteome Software Inc., Portland, ME) was used to validate MS/MS-based peptide and protein identifications. Mascot was set up to search both the forward and reversed sequences of the SwissProt_57.8 database (selected for Humans) assuming the digestion enzyme trypsin (1 missed cleavage allowed), mass tolerance of 1.00 Da and a parent ion tolerance of 2.0 ppm. Carbamidomethylation of cysteine was specified as a

fixed modification and deamidation of asparagine and oxidation of methionine were set as variable modifications in both search engines. Peptide identifications were accepted if they could be established at greater than 95.0%. Protein identifications were accepted if established at greater than 99.9% probability with at least 2 identified peptides. Identified proteins were quantified using spectral counts directly computed by Scaffold and the number of MS/MS spectra were grouped into "counts" associated to a specific protein. Spectral counts normalization was performed by Scaffold 8 version 3_00_02 (Proteome Software Inc.). Subsequently estimation of differential protein abundance was expressed as fold-change (ratio of the averaged spectral counts in the treated cells to the averaged spectral counts in the untreated cells). The normalized spectral count for each identified protein were submitted to SIMCA-P13 software package (Umetrics, Umea, Sweden) for multivariate data analysis (OPLS-DA). Variables that had significant contribution to discrimination between groups and a significant p-value (Mann-Whitney-Wilcoxon test, $p<0.05$), computed using JMP v6 software (SAS Institute, Inc., Cary, NC), were accepted as significantly modulated proteins upon treatment and submitted to network analysis. Functional interpretation of the differentially expressed proteins highlighted by proteomics was built using the MetaCore analytical suite version 5.3 (GeneGo, St. Joseph, MI).

cDNA microarray and RT-PCR analyses

Total RNA was extracted from cells using the Qiagen RNeasy Plus mini kit (Qiagen, Hilden, Germany) according to the supplier's instructions. For the integrity measurement, 4 µl of the total RNA were analyzed on an Agilent Cary 60 UV-Vis Spectrophotometer (Agilent Technologies Inc). Microarray analyses was performed at the Qiagen SuperArray core facility (http://www.sabiosciences.com/customservice_pcrarray.php; SABiosciences, Qiagen, Hilden, Germany). To efficiently retro-transcribed mRNA, the Service Core uses the Qiagen RT² First Strand Kit (Qiagen); the cDNA was then hybridized with customized cDNA microarrays containing specific primers sets for 84 relevant apoptosis genes, cell cycle regulation genes or mitochondrial energy metabolism genes, plus five housekeeping genes. Analysis of gene expression was done essentially as described (available at http://www.sabiosciences.com/customservice_pcrarray.php). A set of controls present on each array enables data analysis using the ΔΔCT method of relative quantification, assessment of reverse transcription performance, genomic DNA contamination, and PCR performance. Alterations due to the treatment on the basal gene expression were determined as the ratio of relative gene expression compared with unstimulated cells and were considered significant when a > 2- or < -2 fold change of modulation was observed. The mitochondrial pathway

activity score was calculated using the bioinformatics tool provided by QIAGEN (available at http://www.sabiosciences.com/dataanalysis.php). Probability score >0,3 or <-0,3 indicates significant change in experimental sample as compared to control sample.

RNA analyses

Total RNA was extracted from cells using the QIAGEN RNeasy Plus mini kit (QIAGEN, Hilden, Germany) according to the supplier's instructions. Once verified the quality of RNA preparation by agarose gel, total RNA was transcribed into cDNA, using the QuantiTect® Reverse Transcription kit (SABiosciences, QIAGEN). *p21*, *MDM2*, *BAX*, *PUMA*, *TIGAR* gene expression was analyzed using the SYBR Green-based real-time quantitative polymerase chain reaction (RT qPCR) detection method with SABiosciences RT^2 Real- Time™ Gene expression assays, which include specific validated primer sets and PCR master mix (SABiosciences). All samples were run in triplicate using the real-time thermal analyzer Rotor-GeneTM 6000 (Corbett, Cambridge, UK). Expression values were normalized to the housekeeping gene *POLR2A* amplified in the same sample.

Transfection experiments

A pool of three specific small interfering RNA (siRNA) for each gene was resuspended in nuclease-free sterile water. Leukemic cells ($2x10^6$ cells/0.1 ml) were mixed with either 1 µg of control enhanced green fluorescence protein (EGFP) plasmid or 3 µg of small interfering RNA (siRNA) cocktails, transferred to a 2.0-mm electroporation cuvette and nucleofected with the nucleofector kit V (Lonza Cologne AG, Cologne, Germany) using the nucleofector device (Amaxa Nucleofector II apparatus, Lonza). After electroporation, cells were immediately transferred to a complete medium and cultured at 37°C until analysis. Transfection efficiency was monitored in each experiment by scoring the percentage of EGFP-positive cells by flow cytometry analysis. For specific gene knock-down, siRNAs were designed and manufactured by Ambion® (Life Technologies) according to the current guidelines for effective gene knock-down by this method. Negative control siRNA consisted of a 19 bp-scrambled sequence with 3' dT overhangs (Ambion's Silencer negative control siRNA). The Ambion's Silencer negative control siRNA sequence has no significant homology to any known gene sequences from human and it has been previously tested for the lack of non-specific effects on gene expression.

Statistical analysis and assessment of the effect of combination treatment

Descriptive statistics were calculated. For each set of experiments (ie, assays for cell cytotoxicity/functionality and RT-analysis), values were reported as means±standard deviation (SD). The results were analyzed by using the Mann-Whitney rank-sum test and statistical significance was defined as $p<0.05$. All statistical analyses were performed with SPSS Statistic 20 software (SPSS Inc., Chicago, IL). In order to investigate the effect of DCA+Nutlin-3 combination, leukemic cells were then treated with serial doses of DCA (range 3-30 mM) or Nutlin-3 (range 1-10 microM), individually or in combination using a constant ratio (DCA:Nutlin-3). Results were analyzed with the method of Chou and Talalay to determine whether combined treatment yields greater effects than expected from summation alone: a combination index (CI) of 1 indicates an additive effect, while a CI below 1 indicates synergism. For this purpose cell viability data were analyzed with the CalcuSyn software (Biosoft, Cambridge, UK) and reported either as CI values or as dose-effect curves directly drawn by the CalcuSyn software. Proteomics data were analyzed by both multivariate and univariate approaches. The normalized spectral counts for each identified proteins were submitted to SIMCA-P13 software package (Umetrics, Umea, Sweden) for multivariate data analysis. Variables were scaled using Pareto scaling and data were analyzed by orthogonal partial least-squares discriminant analysis (OPLS-DA). S-plots were calculated to visualize the relationship between covariance and correlation within the OPLS-DA results. Variables that showed significant contribution to discrimination between groups and a significant change in their expression (Mann-Whitney-Wilcoxon test, $p<0.05$), were accepted as significantly modulated proteins upon treatment and submitted to network analysis.

Results

DCA promotes cytotoxicity in primary B-CLL patient derived cells, but not in normal peripheral blood cells

The first group of experiments was designed to investigate whether DCA promoted cytotoxicity in leukemic cells. For this purpose, the effect of DCA was comparatively analyzed on primary PBMC derived from B-CLL patients (n=22; Table 2) and from healthy blood donors (n=10). Treatment with DCA, used in the range of 1-30 mM for up to 48 hours, exhibited a dose- and time-dependent cytotoxicity, resulting in significant reduction of leukemic cell viability with respect to the untreated cultures, at concentrations ≥3 mM in B-CLL patient cell samples (Figure 3A). The IC_{50} (50% inhibition concentration) mean values (±SD) of cytotoxicity of DCA in B-CLL patient samples were 22±11 mM and 12±6 mM at 24 and 48 hours of treatment, respectively (Figure 3B). On the other hand, PBMC obtained from healthy donors were significantly less susceptible to DCA cytotoxicity as compared to primary B-CLL cells, with IC_{50} mean values (±SD) of cytotoxicity of 122±49 mM and 93±52 mM at 24 and 48 hours of treatment (Figure 3A-B), clearly showing that normal PBMC were completely resistant to DCA effects at concentrations ≤10 mM. Thus, in line with previous data obtained in solid tumor cell models [**95-104**] and multiple myeloma [**105**], we have demonstrated for the first time that DCA promoted a significant cytotoxicity also in primary B-CLL samples but not in normal PBMC.

Table 2. Clinical and laboratory features of the B-CLL patients involved in the study

Patient #	*Age/Sex*	*Rai stage*	*WBC count ($x10^3$/mL)*	*%CD38$^+$ cells*	*ZAP-70*	*IgVH status*	*Cytogenetic abnormalities (FISH)*	*p53 status*	*Therapy*
1	77/M	0	81.4	2	2	mut	del13q omoz.	WT	none
2	85/F	1	54	1	5	mut	tri12	WT	Chl
3	68/M	0	82.9	3.3	21	mut	del13q	na	none
4	79/F	1	47.9	2.9	na	na	na	na	FCR
5	75/F	1	56.6	1.9	8	mut	na	na	none
6	73/F	1	95	2.1	50	mut	del13q	WT	Chl
7	75/M	0	96.8	1.1	30	mut	del13q	WT	none
8	79/F	0	54.8	6.3	1.8	unmut	del11q/del13q omoz.	WT	F
9	66/M	0	108.1	0	24.3	unmut	del13q	WT	FCR
10	56/M	II	128.3	1.2	60	unmut	Normal	WT	FCR
11	82/F	0	23.3	50.9	6.4	mut	Normal	WT	none
12	55/F	0	9.3	77.9	13	unmut	del11q	WT	none
13	65/M	0	25.3	6	27.1	mut	Normal	WT	none
14	75/M	0	23.1	21	19.7	unmut	del13q	WT	none
15	73/M	0	27.7	10.3	10.2	mut	del13q	WT	none
16	71/F	0	14.2	0	20.6	na	del13q	WT	none
17	75/M	0	59.7	6.8	0.3	mut	del13q	WT	none
18	55/F	0	86.5	7	7.4	unmut	del13q	WT	none
19	77/M	IV	100	15.4	72.1	unmut	tris 12	WT	Chl
20	51/F	0	105	2.8	20	unmut	del11q/del13q	WT	none
21	87/F	II	121	58.5	2.4	unmut	del13q/tris 12	WT	Chl
22	72/M	II	21.2	55.2	na	unmut	del13q/tris 12	WT	none

FCR, fludarabine, cyclophosphamide, rituximab; Chl, chlorambucil; mut, mutated; unmut, unmutated; WT, wild-type; na, not available.

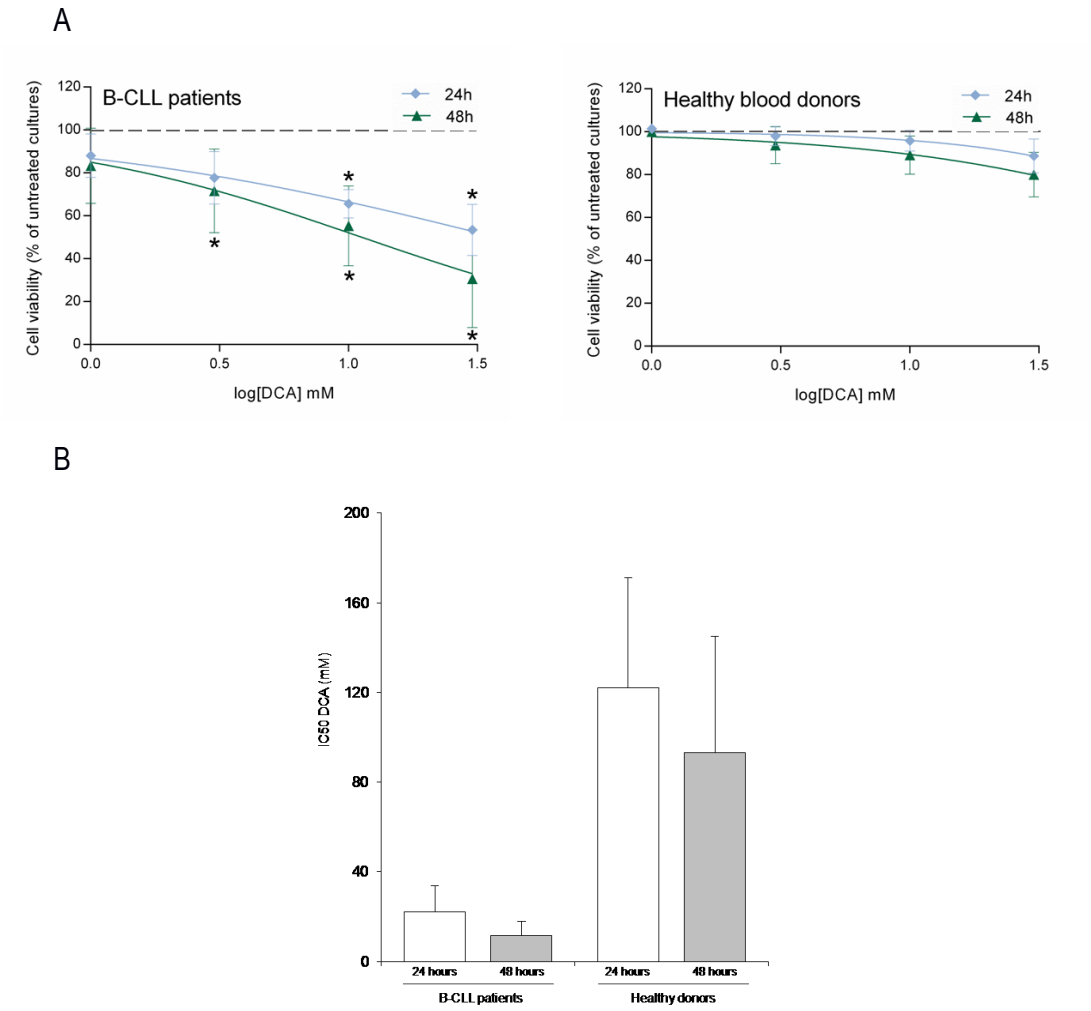

Figure 3. Comparative evaluation of cell viability in response to DCA in B-CLL patient leukemic cells and PBMC from healthy human blood donors. B-CLL patient cell samples (n=22) and PBMC from healthy blood donors (n=10) were exposed to serial doses of DCA (range 1-30 mM) as indicated. In A, cell viability was analyzed at 24 and 48 hours of treatment and was calculated as percentage of untreated cultures set to 100%. Data are reported as mean values ±SD. The asterisk indicates $p<0.05$ with respect to the untreated cultures. In B, IC_{50} values are reported as mean value ±SD.

DCA activates the p53 pathway in p53$^{wild\text{-}type}$ B leukemic cell lines

Most B-CLL at diagnosis are p53$^{wild\text{-}type}$ [**29,30**], as the primary B-CLL samples analyzed in this study, and it is noteworthy that previous studies on solid tumors have implicated the p53 pathway in mediating the anti-tumoral activity of DCA [**96,97,138**]. Therefore, in order to investigate the potential involvement of p53 in mediating the anti-leukemic activity of DCA, we next performed a series of experiments on three p53$^{wild\text{-}type}$ B leukemic cell lines (EHEB, JVM-2 and JVM-3). As shown in Figure 4A, treatment with DCA resulted in a dose-dependent reduction of cell viability in all the p53$^{wild\text{-}type}$ B leukemic cell lines tested; accordingly the IC_{50} values varied from 30.9 to 46.5 mM at 24 hours of treatment and from 13.8 to 19.5 mM at 48 hours of treatment, comparable to those of primary B-CLL cells (Figure 3B). Flow cytometric analysis of these leukemic cell cultures demonstrated that treatment with DCA induced early accumulation in G1 phase of the cell cycle (Figure 4B) and promoted apoptosis in all leukemic cell lines (Figure 4C). The cytotoxic effects of DCA on the B cell lines were coupled to the ability of DCA to reduce the mitochondrial membrane potential (Figure 4D).

A

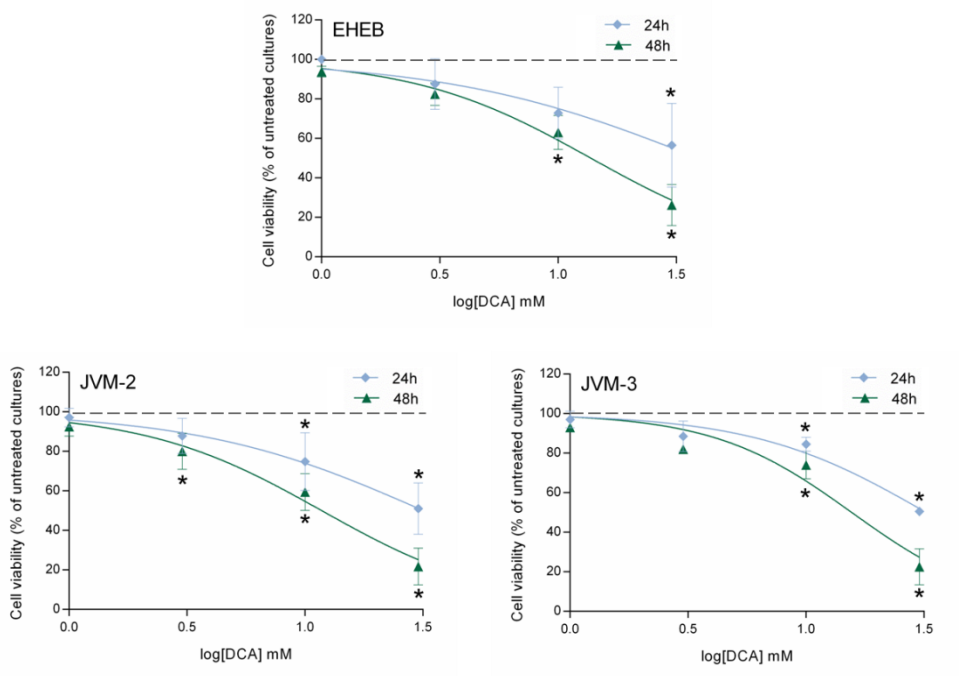

B

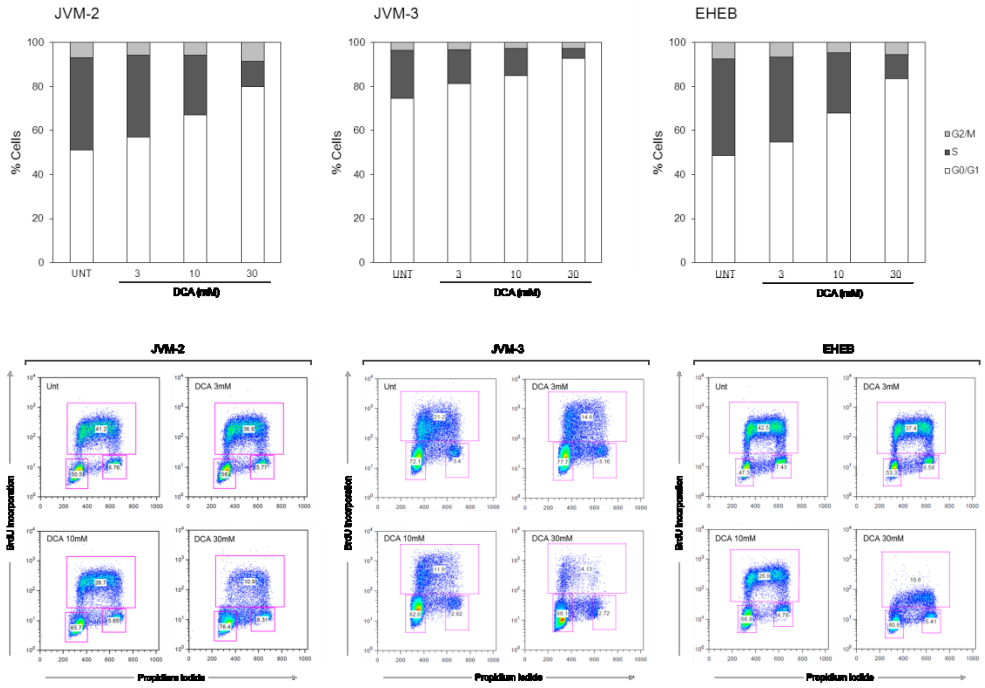
JVM-2
JVM-3
EHEB
% Cells
UNT
3
10
30
DCA (mM)
G2/M
S
G0/G1
BrdU Incorporation
Propidium Iodide
Unt
DCA 3mM
DCA 10mM
DCA 30mM

C

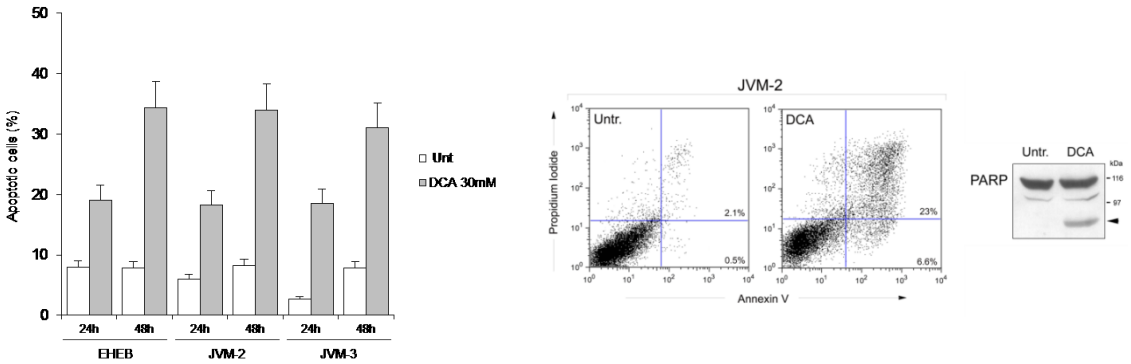
Apoptotic cells (%)
Unt
DCA 30mM
24h
48h
EHEB
JVM-2
JVM-3
JVM-2
Untr.
DCA
Propidium Iodide
Annexin V
2.1%
0.5%
23%
6.6%
PARP
Untr.
DCA
kDa
116
97

D

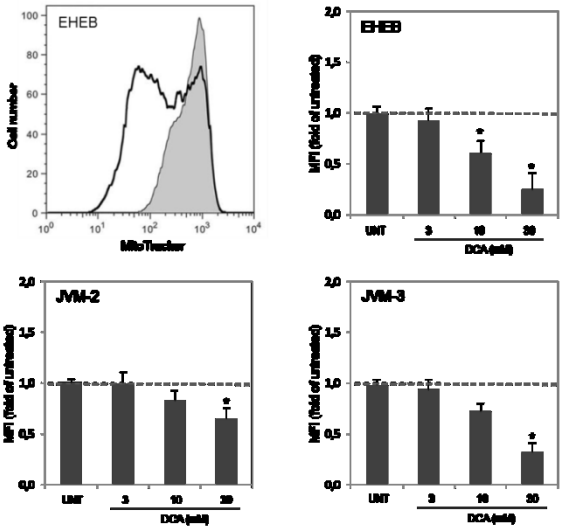
EHEB
Cell number
MitoTracker
MFI (fold of untreated)
UNT
3
10
30
DCA (mM)
JVM-2
JVM-3

Figure 4. Cytotoxicity induced by DCA in B leukemic cell lines. The $p53^{wild\text{-}type}$ (EHEB, JVM-2, JVM-3) B leukemic cell lines were exposed to DCA before analysis of cell toxicity. In A, cell viability in response to serial doses of DCA (range 1-30 mM), was calculated at both 24 and 48 hours of treatment as percentage with respect to the control vehicle cultures (set to 100% for each cell line). In B, cell distribution in the different phases of cell cycle was calculated from the flow cytometry dot plots after BrdU/PI staining and expressed as percentage of the total population. Representative cell-cycle profiles of cells, either left untreated or treated with serial doses of DCA, analyzed by flow cytometry are shown. In the right panel, the rectangles represent the cells in G0/G1, S, G2/M phases of the cell cycle. In C, the percentage of apoptotic cells was determined by flow-cytometry after Annexin V/PI staining (upper panel). A representative flow cytometric analysis of apoptosis, validated also by Western blot analysis of PARP cleavage, is shown (lower panels). In D, to measure changes in the mitochondrial membrane potential ($\Delta\psi_m$), upon treatment with DCA for 24h cells were stained with MitoTracker solution and analyzed by flow cytometry. Median values of mitochondrial MitoTracker fluorescence and representative histograms are shown. In A, C and D, data are reported as the mean±SD of results from three independent experiments. In A and D, the asterisk indicates $p<0.05$ with respect to the untreated cultures of each cell line.

Based on these evidences, documenting the anti-proliferative/pro-apoptotic activity of DCA in B leukemic cells, we next assessed the effect of DCA treatment on the expression of p53 in the EHEB, JVM-2, JVM-3 cell lines by two-dimensional electrophoresis and immunoblotting, which allows separation of proteins based on their molecular weight (MW) and isoelectric point (pI). As shown in Figure 5A, two-dimensional electrophoresis revealed the presence of the full-length p53 (~53 kDa, pI 6-7.3) beside a group of spots below the 53 kDa (~40 kDa, pI 5.5-6.5) in the untreated cultures. Upon DCA treatment for 24 hours, we observed a slight increase in the full-length p53 protein in the EHEB cell line and, of note, the appearance of a series of isoforms above the 53 kDa in all the cell lines, suggestive of p53 post-translational modifications. In this respect, in Western blot assay we have documented that DCA dose-dependently induced p53 phosphorylation in Ser^{15} and Ser^{392} (Figure 5B). To test the hypothesis of functional activation of p53 upon exposure to DCA, in parallel experiments we have analyzed the levels of a subset of p53 transcriptional targets involved in promoting cell cycle arrest (p21), modulation of apoptosis (MDM2, Bax, PUMA) or metabolism (TIGAR) by RT-PCR. As shown in Figure 3C, DCA variably but significantly (>2 fold) increased the mRNA levels of *MDM2*, *p21*, *PUMA* and *TIGAR* in all leukemic cell lines investigated, while no significant modulation of *BAX* mRNA was observed.

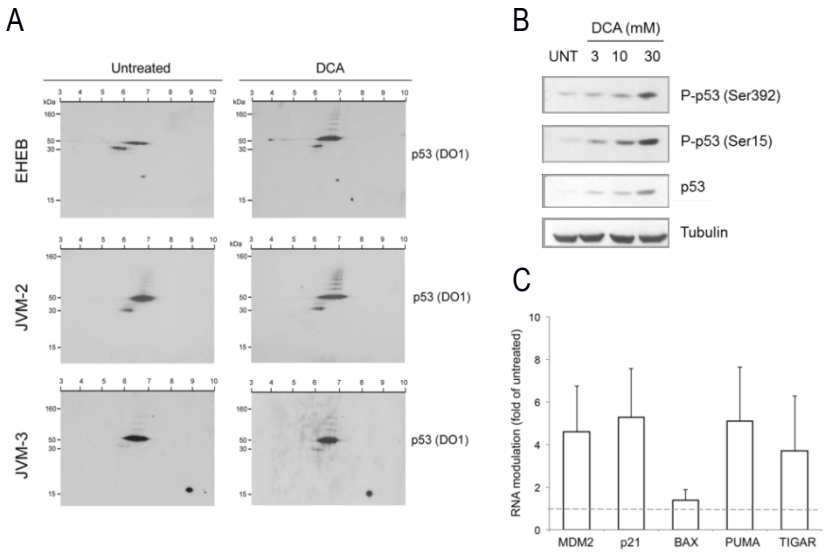

Figure 5. Activation of p53 pathway by DCA in $p53^{wild\text{-}type}$ B leukemic cells. $p53^{wild\text{-}type}$ B leukemic EHEB, JVM-2 and JVM-3 cells were left untreated or treated with DCA for 24 hours. In A, cell lysates were analyzed by two-dimensional immunoblot. The antibody p53 (DO-1) identified a spot group corresponding to full-length p53 (~53 kDa) and a series of p53 isoforms with a molecular weight above 53 kDa (square brackets). In B, equal amounts of cell lysates, obtained from EHEB cells, were analyzed for protein levels by Western blot. Tubulin staining is shown as a loading control. Blots representative of at least three independent experiments yielding equivalent results are shown. In C, transcriptional activation of p53 target genes, *MDM2*, *p21*, *BAX*, *PUMA* and *TIGAR*, was assessed by quantitative RT-PCR. mRNA levels are expressed as folds of modulation, with respect to the control untreated cultures set at 1. Results are reported as means±SD of six independent experiments carried out on the three different cell lines.

DCA plus Nutlin-3 combination exhibits a potent synergistic anti-leukemic activity

In the next group of experiments, we have examined the potential interaction of DCA with Nutlin-3, a small molecule which transcriptionally activates p53 by abolishing its interaction with its principal inhibitor MDM2 [**139**]. For this purpose, leukemic cells were treated with DCA (3-30 mM) and Nutlin-3 (1-10 μM), used as single agents and in combination. In particular, B-CLL leukemic cells were treated with serial concentrations of DCA and Nutlin-3 at a constant DCA:Nutlin-3 ratio for data analysis by the method of Chou and Talalay. Combined treatment with DCA+Nutlin-3 resulted in significantly ($p<0.01$) greater cytotoxicity with respect to the single agents, with a synergistic effect both in primary B-CLL patient samples as well as in B leukemic cell lines (Figure 6A-B), as documented by an average Combination Index (CI) <1 (Table 3). The cytotoxicity induced by the combined treatment with DCA+Nutlin-3 was mainly due to the increase of the degree of apoptosis with respect to the treatment with DCA or Nutlin-3 used alone (Figure 6C).

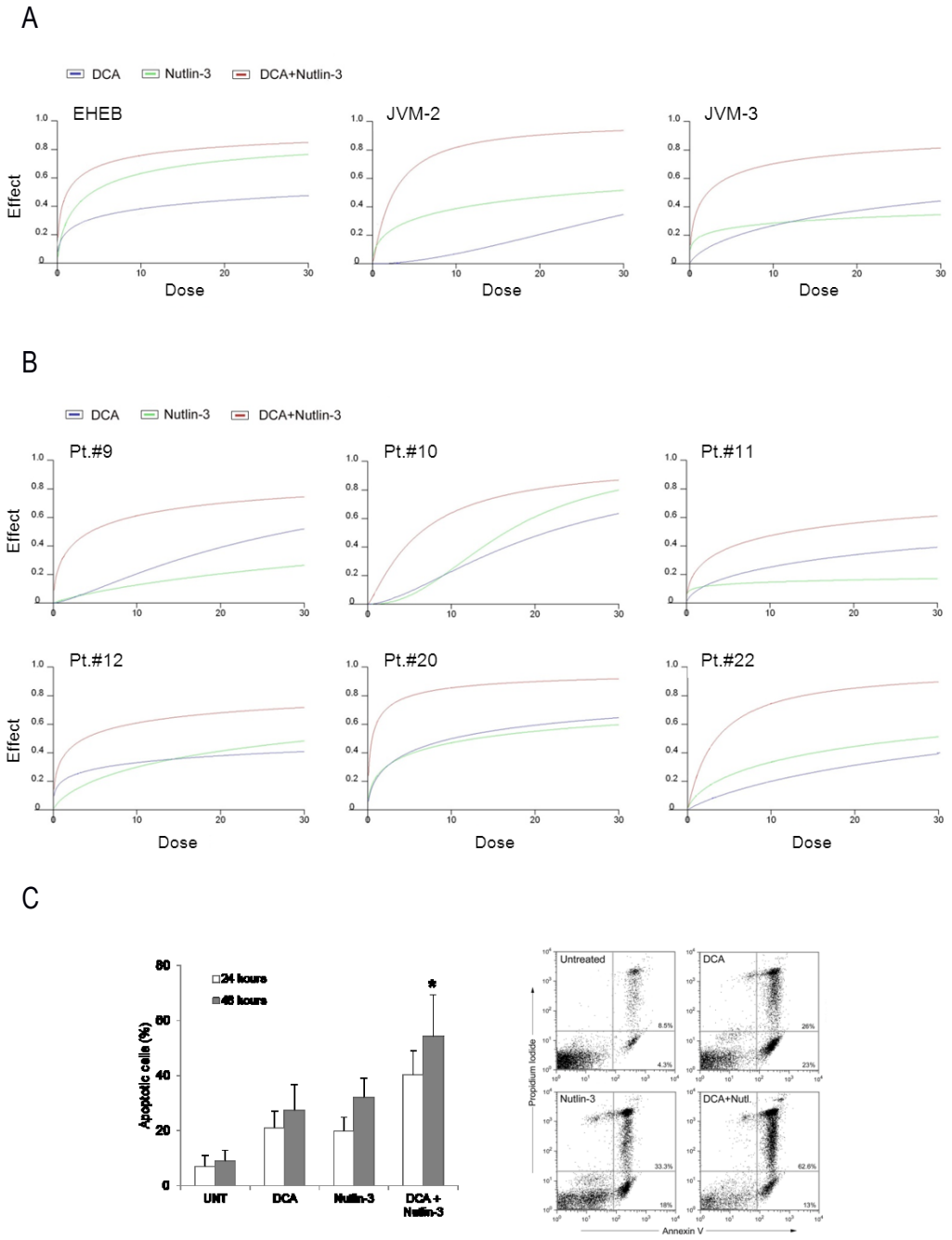

Figure 6. Cytotoxicity by DCA and Nutlin-3 used alone or in combination in p53$^{wild\text{-}type}$ B leukemic cells and B-CLL patient leukemic cells. p53$^{wild\text{-}type}$ B leukemic EHEB, JVM-2 and JVM-3 cells and B-CLL patient leukemic cells were exposed to serial doses of DCA or Nutlin-3 used either alone or in combination, with a fixed ratio, for 24 hours. Dose-effect plots, to determine drug efficacy, are shown for each cell line (A) and for representative B-CLL patient samples (B). The decrease of cell viability, labeled "effect" on the Y-axis, was determined in assays done at least twice in duplicate. In C, induction of apoptosis in B-CLL patient leukemic cells was calculated as percentage of Annexin V/PI cells. Data are reported as mean±SD of results from three independent experiments. A representative flow cytometric analysis of apoptosis in a primary B-CLL sample is shown. The asterisk indicates $p<0.05$ with respect to cultures treated with either DCA or Nutlin-3 alone.

Table 3. Combination index values for the effect of DCA plus Nutlin-3 on viability of B-CLL patient cells and $p53^{wild\text{-}type}$ B cell lines

Cells	*ED50*	*ED75*	*ED90*	*Average CI*
Patient #1	0.33	0.29	0.26	0.29
Patient #2	0.18	0.03	0.01	0.07
Patient #3	0.37	0.38	0.40	0.38
Patient #4	0.31	0.39	0.52	0.41
Patient #5	0.43	0.37	0.34	0.38
Patient #6	0.37	0.31	0.30	0.33
Patient #7	0.37	0.32	0.29	0.33
Patient #8	0.06	0.16	0.46	0.23
Patient #9	0.20	0.56	1.61	0.79
Patient #10	0.67	0.95	1.36	0.99
Patient #11	0.20	0.27	0.37	0.28
Patient #12	0.15	0.29	0.68	0.37
Patient #13	0.05	0.06	0.09	0.07
Patient #14	0.19	0.02	0.004	0.07
Patient #15	0.35	0.1	0.03	0.16
Patient #16	0.24	0.04	0.007	0.10
Patient #17	0.11	0.30	0.80	0.40
Patient #18	0.45	0.43	0.42	0.43
Patient #19	0.01	0.08	0.58	0.22
Patient #20	0.09	0.07	0.05	0.07
Patient #21	0.22	0.24	0.29	0.25
Patient #22	0.19	0.13	0.09	0.14
EHEB	0.39	0.49	0.66	0.51
JVM-2	0.16	0.11	0.13	0.13
JVM-3	0.06	0.08	0.11	0.08

ED indicates effect dose. The average combination index (CI) values were calculated from ED50, ED75, and ED90.

Role of p21 induction in DCA and DCA+Nutlin-3 induced cytotoxicity in leukemic cells

With respect to DCA treatment, Nutlin-3 induced a much more potent accumulation of both p53 and its molecular targets MDM2 and p21 in $p53^{wild\text{-}type}$ leukemic cells, as documented by Western blot analysis performed on total cell lysates (Figure 7A). The combination of DCA+Nutlin-3 did not result in a further accumulation of p53 protein with respect to Nutlin-3 alone while it promoted a greater induction of MDM2 and p21 proteins with respect to Nutlin-3 alone (Figure 7A). Interestingly, the combination of Nutlin-3+DCA significantly ($p<0.05$) enhanced the induction of *MDM2* and *p21* at the mRNA level, in both B leukemic cell lines and primary B-CLL patient samples, but not in normal PBMC (Figure 7B). Of note, the synergistic transcriptional induction of p53-target

genes by DCA+Nutlin-3, documented in leukemic cells but not in normal PBMC, correlated with the lower cytotoxicity of DCA+Nutlin-3 in these cells (Figure 7C).

A

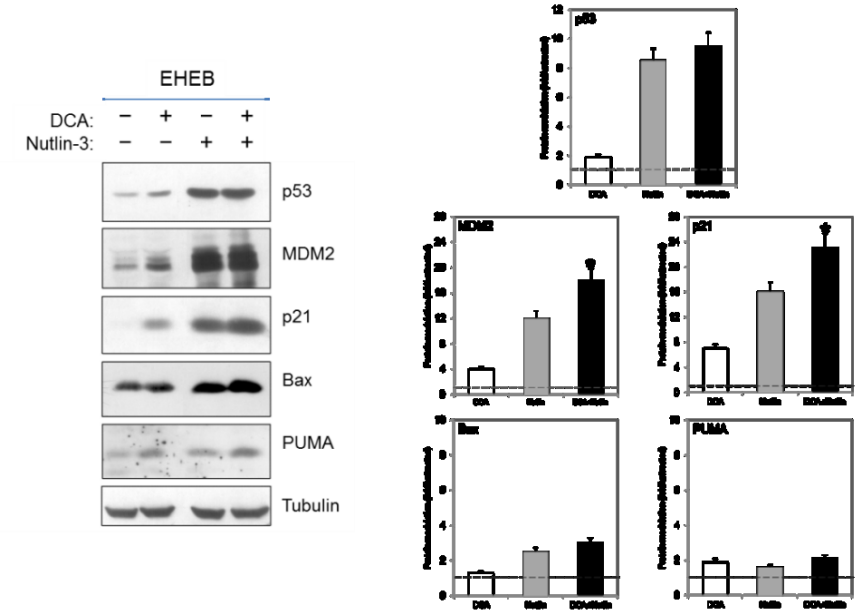

B

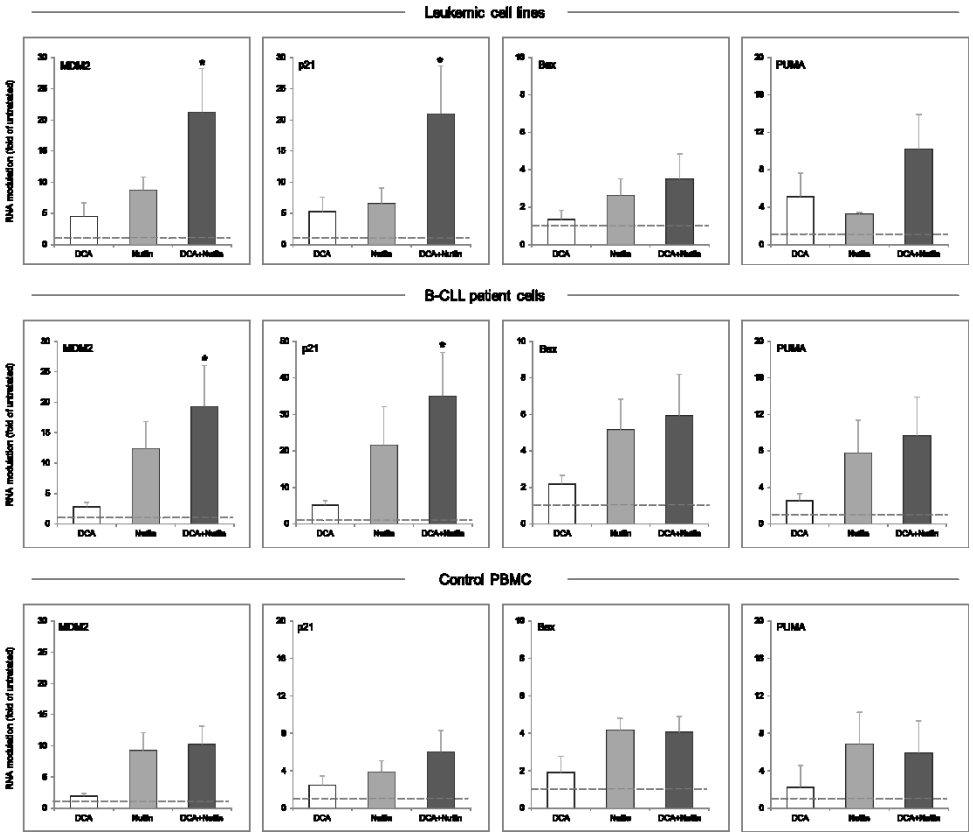

C

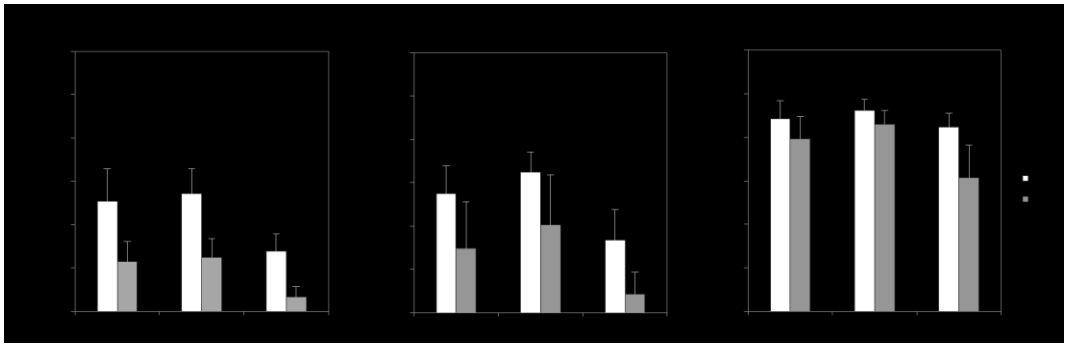

Figure 7. Activation of p53 pathway by DCA+Nutlin-3 combination. In A, equal amounts of cell lysates, obtained from EHEB cells treated for 24 hours with DCA and Nutlin-3, used either alone or in combination, were analyzed for protein levels by Western blot. Tubulin staining is shown as a loading control. Blots representative of at least three independent experiments yielding equivalent results are shown. After densitometric analyses, protein levels are expressed as folds of protein modulation, by the indicated treatments, with respect to the control untreated cultures set at 1. In B and C, $p53^{wild\text{-}type}$ B leukemic cell lines, B-CLL patient leukemic cells and PBMC from healthy human blood donors respectively were exposed for 24 hours to DCA and Nutlin-3, used either alone or in combination, as indicated. In B, the expression levels of p53 target genes were assessed by quantitative RT-PCR and results were indicated as folds of modulation with respect to the control untreated cultures set at 1. Data are reported as mean±SD of results from independent experiments. The asterisk indicates $p<0.05$ with respect to cultures treated with either DCA or Nutlin-3 alone. In C, cell viability was analyzed at 24 and 48 hours of treatment and was calculated as percentage of untreated cultures set to 100%. Data are reported as mean values ±SD.

The data illustrated above demonstrated that DCA+Nutlin-3 strongly synergized both in promoting leukemic cytotoxicity as well as in inducing p53 transcriptional activity; it was particularly noteworthy that one of the genes up-regulated in response to DCA±Nutlin-3 was *p21*. In this respect, a recent study has demonstrated that a strong induction of p21 by genotoxic agents was predictive of better prognosis in B-CLL [**140**]. Conversely, a lack of induction of p21 was observed in B-CLL patient samples showing a worse prognosis even in the presence of an integral activation of p53 [40]. Therefore, in order to functionally elucidate the role of p21 in mediating the anti-leukemic activity of DCA+Nutlin-3, we utilized siRNAs to attenuate p21 expression. The knock-down of *p21* expression was demonstrated by quantitative RT-PCR, documenting a significant reduction of *p21* mRNA in EHEB cells, transfected with a cocktail of p21 specific siRNAs, both at baseline as well as after DCA+Nutlin-3 treatment (Figure 8A). Of note, in EHEB samples in which p21 expression was knocked-down by transfection with p21 specific siRNAs, the DCA+Nutlin-3-mediated cytotoxicity was significantly ($p<0.05$) reduced with respect to either cells transfected with a scrambled control siRNA

or cells not transfected (Figure 8B). Overall, these experiments support a potential role of p21 in modulating the anti-leukemic activity of DCA+Nutlin-3.

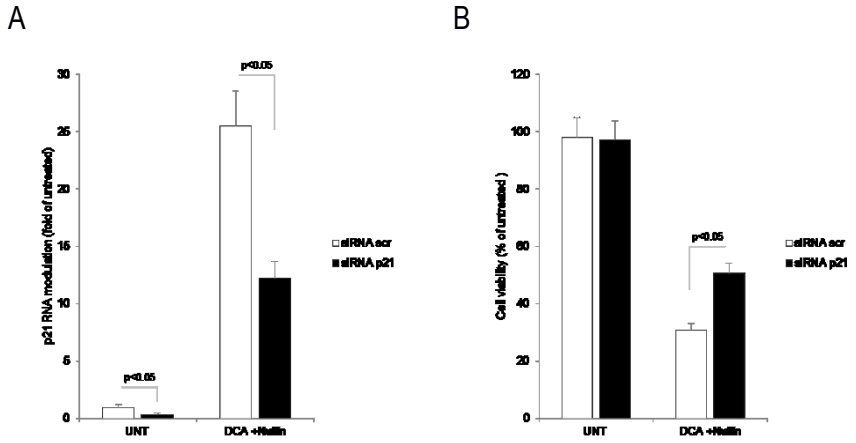

Figure 8. Role of p21 pathway in mediating the anti-leukemic activity of DCA+Nutlin-3. EHEB cells were transfected with either control scrambled (scr) siRNA or p21 siRNA before treatment. In A, after transfection, efficiency of p21 knock-down was documented by analyzing levels of *p21* mRNA by quantitative RT-PCR, in untreated cells and upon treatment with DCA+Nutlin-3. Results are expressed as folds of modulation with respect to the control cultures. In B, cultures transfected with either control scrambled (scr) siRNA or p21 siRNA were analyzed for cell viability upon exposure to DCA+Nutlin-3. Results are expressed as percentage with respect to the control vehicle cultures (set to 100%). Data are reported as means±SD.

DCA promotes comparable cytotoxicity in p53$^{wild\text{-}type}$ and p53^{mutated} B-CLL patient cells

Since B-CLL patients characterized by p53 dysfunction have limited treatment options and poor overall survival [**129,131,132**], we then comparatively evaluated the *in vitro* effect of DCA assessed on B-CLL patient cells characterized by either p53 wild-type or harboring TP53 mutations (Table 4). For this purpose, upon validation of a TP53 next generation sequencing screening (performed on a total of 80 B-CLL patients), we selected 5 patients with p53 wild-type and 5 patients characterized by mutations potentially affecting p53 functionality, as predicted by web mutation pathogenicity prediction tools and protein structural bioinformatic analysis (Table 4 and Figure 9). B-CLL cell cultures were exposed *in vitro* to DCA in a range of concentrations (1-30 mM) previously used by other authors in *in vitro* solid tumor models [**101-103,105**]. As documented by the IC_{50} values, *in vitro* treatment with DCA induced a significant and progressive reduction of cell viability, with respect to the untreated cultures assessed at the same time points (24 and 48 hours), in all the primary B-CLL patient cell cultures, irrespectively of the p53 status (Table 5).

Table 4. Clinical and laboratory characteristics of selected B-CLL patients

B-CLL Pt.#	*Sex*	*Age*	*Rai stage*	*Therapy*	*%CD38+ cells*	*%ZAP-70+*	*Cytogenetic Abnormalities**	*IgVH status*	*TP53 analysis (NGS)*
1	M	73	0	none	10.3	10.2	del13q	mut	unmut
2	F	78	0	F	6.3	1.8	del11q/del13q omoz.	unmut	unmut
3	M	63	0	FCR	0	24.3	del13q	unmut	unmut
4	M	54	II	FCR	1.2	60	normal	unmut	unmut
5	M	77	IV	Chl	15.4	72.1	tris 12	unmut	unmut
6	M	55	0	FCR	6.7	18.9	tris 12	unmut	NM_000546:exon5:c.470T>A:p.V157D
7	M	71	IV	FCR	6.5	na	del13q/del17p	mut	NM_000546:exon8:c.817C>T:p.R273C NM_000546:exon7:c.701A>G:p.Y234C
8	M	68	IV	R-Benda	16.6	8.6	del11q/del13q/del17p	unmut	NM_000546:exon7:c.770T>C:p.L257P
9	M	79	II	Chl	14.3	1.9	del13q/del17p	unmut	NM_000546:exon6:c.376-2A>G: p.Y126Tfs*44
10	M	75	0	Chl	3.6	41.1	del13q/del17p	na	NM_000546:exon8:c.832C>T:p.P278S

Pt., patient; NGS, next generation sequencing; mut, mutated; unmut, unmutated; na, not available; F, Fludarabine; FCR, Fludarabine-Cyclophosphamide-Rituximab; R-Benda, Rituximab-Bendamustine; Chl, Chlorambucil. * Cytogenetic abnormalities were evaluated by fluorescence in situ hybridization (FISH) analysis.

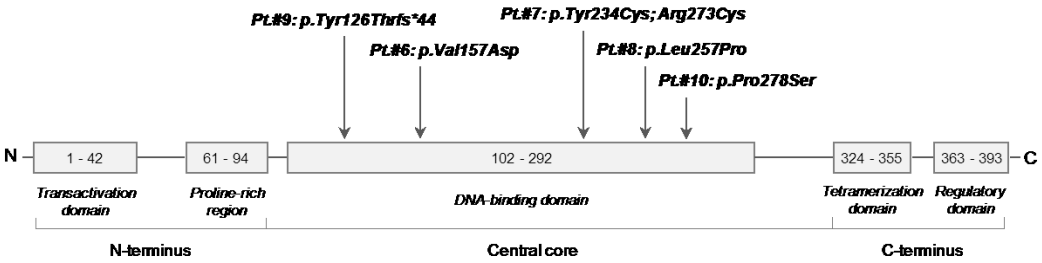

Figure 9. Sites of mutation in p53 in the B-CLL patients investigated. A schematic representation of the 393 amino acid domain structure of human p53 is shown. The sites of the mutations detected in the B-CLL patients (Pt.#6-10) are indicated. The nomenclature follows the current HGVS recommendations for the description of sequence variants.

Table 5. IC50 for DCA in leukemic cells

Leukemic cells	*TP53 status*	*IC50 DCA (mM)*	
		24 hours	*48 hours*
B-CLL Pt.#1	wild-type	20.6	14.7
B-CLL Pt.#2	wild-type	24.8	12.7
B-CLL Pt.#3	wild-type	28.5	9.7
B-CLL Pt.#4	wild-type	23.1	16.5
B-CLL Pt.#5	wild-type	36.2	<1
B-CLL Pt.#6	mutated	41.9	20.4
B-CLL Pt.#7	mutated	32.1	15.0
B-CLL Pt.#8	mutated	5.0	<1
B-CLL Pt.#9	mutated	17.0	15.6
B-CLL Pt.#10	mutated	28.1	14.8
MAVER	mutated	27.9	14.5
MEC-1	mutated	16.2	10.4
MEC-2	mutated	33.7	22.7
HL-60	null	43.0	24.4

Although we have previously shown that DCA activates the p53 pathway in $p53^{wild\text{-}type}$ B leukemic cells, the current set of data suggested that DCA can promotes cytotoxicity also independently of functional p53. Thus, to investigate the molecular mechanisms underlining DCA cytotoxicity in leukemic cells with dysfunctional p53, we selected three $p53^{mutated}$ B leukemic cell lines (MAVER, MEC-1, MEC-2), which exhibited a dose- and time-dependent cytotoxic response to DCA

(Figure 10A) with IC_{50} values comparable to those assessed for primary $p53^{wild\text{-}type}$ and $p53^{mutated}$ B-CLL cells (Table 5). The ability of DCA to promote p53-independent cytotoxicity in leukemic cells was further supported by experiments performed on the $p53^{null}$ HL-60 cell line (Figure 10B).

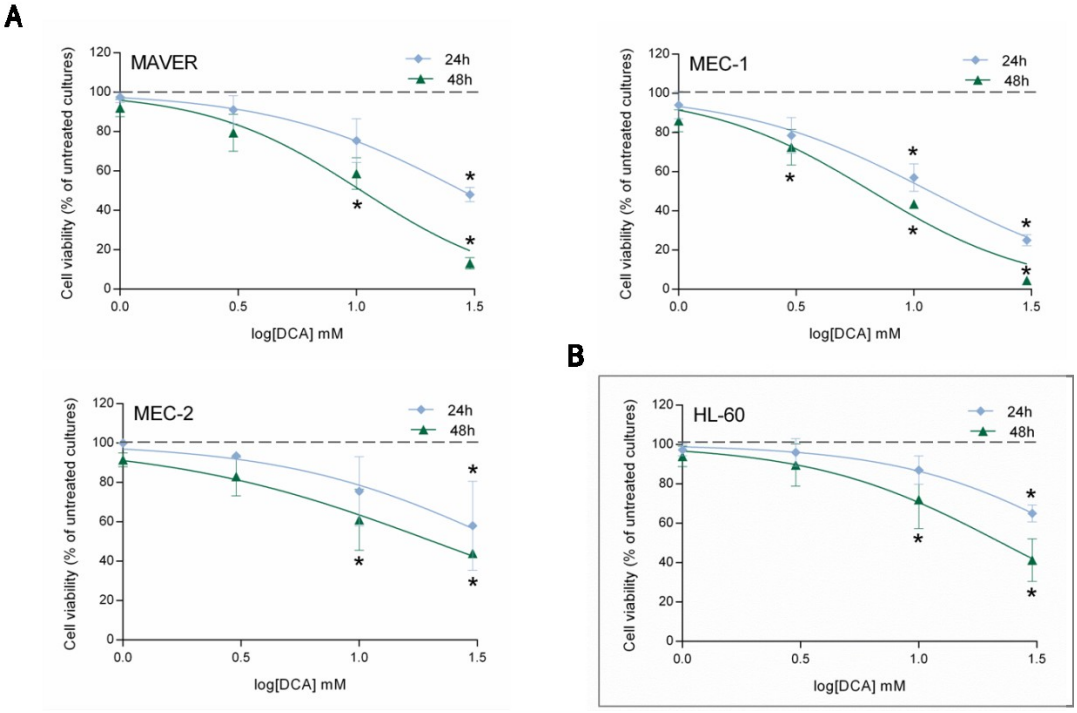

Figure 10. Cytotoxicity induced by DCA in p53mutated/null leukemic cell lines. The $p53^{mutated}$ B leukemic cell lines MAVER, MEC-1 and MEC-2 (A), as well as the p53null HL-60 cells (B), were exposed to serial doses of DCA (range 1-30 mM) before analysis of cell viability at both 24 and 48 hours of treatment. Dose response curves were derived by calculating the cell viability as percentage with respect to the untreated cultures (set to 100%). Data are means±SD of at least three independent experiments, each performed in duplicate (Mann-Whitney rank-sum test; asterisks, $p<0.05$).

The cytotoxicity induced by DCA in $p53^{mutated/null}$ leukemic cell lines was the result of (i) a cytostatic effect with the accumulation in G1 phase of the cell cycle (Figure 11A), (ii) the promotion of cellular senescence (Figure 11B), (iii) the induction of mitochondrial damage as documented by both the morphological remodelling of mitochondrial structure and the reduction in ATP synthesis (Figure 11C), coupled to (iv) apoptosis (Figure 11D).

A

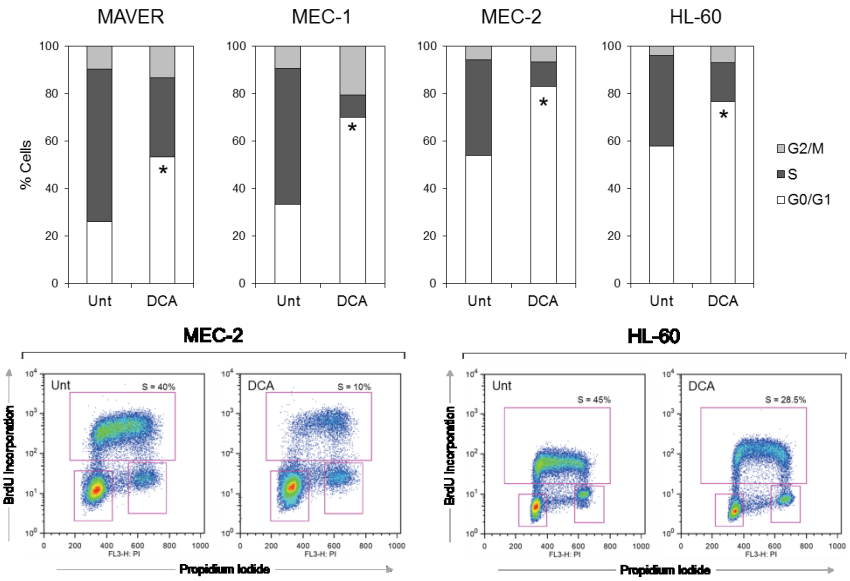
MAVER
MEC-1
MEC-2
HL-60
% Cells
Unt
DCA
G2/M
S
G0/G1
MEC-2
HL-60
Unt
DCA
S = 40%
S = 10%
S = 45%
S = 28.5%
BrdU incorporation
Propidium Iodide
FL3-H: PI

B

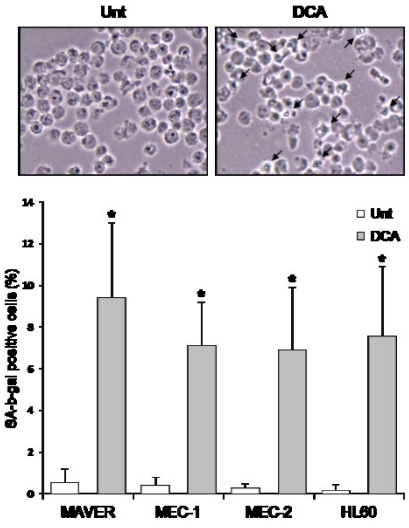
Unt
DCA
SA-b-gal positive cells (%)
MAVER
MEC-1
MEC-2
HL60

C

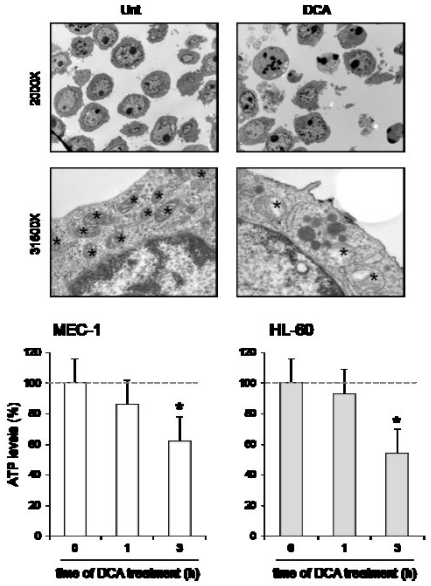
Unt
DCA
2000X
3160X
MEC-1
HL-60
ATP levels (%)
time of DCA treatment (h)

D

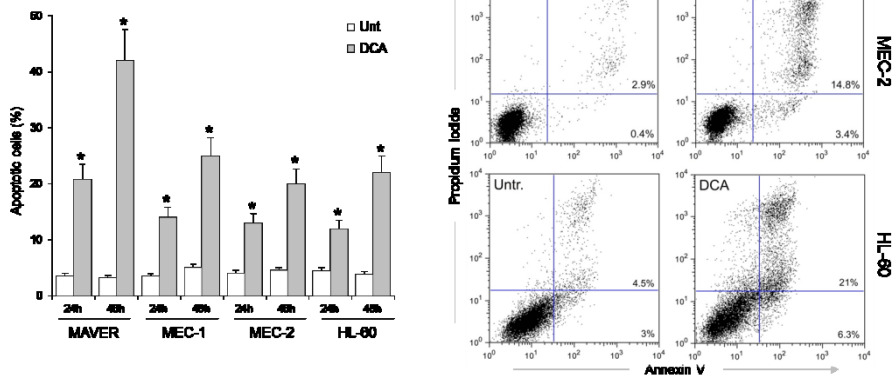
Unt
DCA
Apoptotic cells (%)
24h
48h
MAVER
MEC-1
MEC-2
HL-60
Untr.
DCA
2.9%
0.4%
14.8%
3.4%
4.5%
3%
21%
6.3%
MEC-2
HL-60
Propidium Iodide
Annexin V

Figure 11. Effects of DCA treatment on $p53^{mutated/null}$ leukemic cell lines. The $p53^{mutated}$ B leukemic cell lines MAVER, MEC-1 and MEC-2, as well as the $p53^{null}$ HL-60 cells, were exposed to DCA (30 mM). In A, cell distribution in the different phases of the cell cycle was calculated from the flow cytometry dot plots after BrdU/PI staining and expressed as percentage of the total population. In the upper panel, data are reported as the means of results from at least three independent experiments (Mann-Whitney rank-sum test; asterisks, $p<0.05$). In the lower panel, representative cell cycle profiles of cultures, either left untreated or treated with DCA, analyzed by flow cytometry are shown. For each cytofluorimetric analysis, the rectangles represent the cells in G0/G1, S, G2/M phases of the cell cycle. In B, cell senescence was visualized by SA-β-gal staining. Representative fields observed under light microscope are shown (arrows, senescent cells); cells with positive staining for SA-β-gal were quantified by counting a total of 1000 cells for each culture condition. Data are expressed as means±SD of six different fields in three independent experiments (Mann-Whitney rank-sum test; asterisks, $p<0.05$). In C, assessment of mitochondrial alterations was carried out by morphological and functional analyses. Transmission electron microscopy images of cytosolic regions show mitochondria (asterisks; original magnification 31,500X) with either normal morphology or cristae remodeling, in untreated or DCA treated cultures, respectively. Representative fields of three independent experiments are shown. In the lower panel, cellular ATP levels were quantified in cell lysates at the indicated time points. Data are reported as percentage with respect to the untreated cultures (set to 100%) and are means±SD of three independent experiments, each performed in duplicate (Mann-Whitney rank-sum test; asterisks, $p<0.05$). In D, the percentage of apoptotic cells was determined by flow cytometry after Annexin V/PI staining. Representative experiments are shown. In the graph, data are reported as the means±SD of results from at least three independent experiments (Mann-Whitney rank-sum test; asterisks, $p<0.05$).

DCA effects on HL-60 apoptosis, cell cycle and mitochondrial energy metabolism transcriptomic profile

To address the p53-independent mechanism of DCA action at transcriptional level, we performed a gene expression profile of HL-60 cells exposed to DCA 30mM for 24h in comparison to untreated cells. For this purpose, RNA was analyzed by cDNA microarray for a set of genes, which can be sub-grouped according to their cellular function in apoptosis, cell cycle and mitochondrial energy metabolism-related genes. The analysis evidenced a general up-modulation of apoptotic and cell cycle related-genes and a down-modulation of mitochondrial energy metabolism genes. Genes that were significantly differentially modulated (above the cutoff of 2 fold of induction or below the cutoff of -2 fold of reduction) for each set are reported in Tables 6-8. Among the group of apoptotic genes, DCA induced prevalently the transcription of anti-apoptotic genes, such as BCL2-related proteins (BAG3, BCL2, BCL2A1), the inhibitory factor XIAP and the decoy receptor for TRAIL TNFRSF11B. In parallel, the cell cycle transcriptomic profile is consistent with the anti-mitotic

response of HL-60 cells upon DCA treatment, as evidenced in Figure 11A. Indeed, the microarray analysis revealed the activation of two important genes involved in cell cycle arrest, namely CDKN1A (p21) and CDK5R1 [**141**].

Table 6. Apoptosis-related genes differentially modulated in HL-60 cells after DCA treatment

Description	*Symbol*	*Fold Regulation*
BCL2-associated athanogene 3	BAG3	**8,05**
Baculoviral IAP repeat containing 3	BIRC3	1,50
B-cell CLL/lymphoma 2	BCL2	1,97
BCL2-antagonist/killer 1	BAK1	1,65
BCL2-like 11 (apoptosis facilitator)	BCL2L11	1,60
BCL2-related protein A1	BCL2A1	**2,64**
Bifunctional apoptosis regulator	BFAR	1,53
CASP2 and RIPK1 domain containing adaptor with death domain	CRADD	-1,52
CASP8 and FADD-like apoptosis regulator	CFLAR	1,76
CD27 molecule	CD27	**2,67**
CD40 molecule, TNF receptor superfamily member 5	CD40	1,95
CD70 molecule	CD70	**2,37**
Growth arrest and DNA-damage-inducible, alpha	GADD45A	**2,00**
Lymphotoxin beta receptor (TNFR superfamily, member 3)	LTBR	1,81
Tumor necrosis factor	TNF	**2,53**
Tumor necrosis factor receptor superfamily, member 10b	TNFRSF10B	1,82
Tumor necrosis factor receptor superfamily, member 11b	TNFRSF11B	**5,61**
Tumor necrosis factor receptor superfamily, member 9	TNFRSF9	**3,12**
X-linked inhibitor of apoptosis	XIAP	**2,04**

Data report genes differentially modulated (above the cutoff of 1.5 fold of induction or below the cutoff of -1.5 fold of reduction) after DCA 30mM treatment in HL-60 cells. Genes significantly up-modulated (above the cutoff of 2 fold of induction) or down-modulated (below the cutoff of -2 fold of reduction) are indicated in boldface type.

Table 7. Cell cycle-related genes differentially modulated in HL-60 cells after DCA treatment

Description	*Symbol*	*Fold Regulation*
Ataxia telangiectasia mutated	ATM	1,50
Cell division cycle 34 homolog (S. cerevisiae)	CDC34	**2,04**
Cyclin G2	CCNG2	1,73
Cyclin-dependent kinase 5, regulatory subunit 1 (p35)	CDK5R1	**2,21**
Cyclin-dependent kinase inhibitor 1A (p21, Cip1)	CDKN1A	**3,42**
Cyclin-dependent kinase inhibitor 1B (p27, Kip1)	CDKN1B	1,50
Cyclin-dependent kinase inhibitor 2A (melanoma, p16, inhibits CDK4)	CDKN2A	1,81
Growth arrest and DNA-damage-inducible, alpha	GADD45A	**2,00**
Mdm2 p53 binding protein homolog (mouse)	MDM2	1,75
Minichromosome maintenance complex component 2	MCM2	-1,50
RAD51 homolog (S. cerevisiae)	RAD51	-1,89
SERTA domain containing 1	SERTAD1	**2,62**
S-phase kinase-associated protein 2 (p45)	SKP2	-1,73

Data report genes differentially modulated (above the cutoff of 1.5 fold of induction or below the cutoff of -1.5 fold of reduction) after DCA 30mM treatment in HL-60 cells. Genes significantly up-modulated (above the cutoff of 2 fold of induction) or down-modulated (below the cutoff of -2 fold of reduction) are indicated in boldface type.

Table 8. Mitochondrial energy metabolism-related genes differentially modulated in HL-60 cells after DCA treatment

Description	*Symbol*	*Fold Regulation*
ATP synthase, H+ transporting, mitochondrial Fo complex, subunit C1 (subunit 9)	ATP5G1	-1,54
ATP synthase, H+ transporting, mitochondrial Fo complex, subunit C2 (subunit 9)	ATP5G2	-1,65
Cytochrome c oxidase subunit Vic	COX6C	1,95
NADH dehydrogenase (ubiquinone) 1 alpha subcomplex, 5, 13kDa	NDUFA5	**-3,69**
NADH dehydrogenase (ubiquinone) 1 beta subcomplex, 6, 17kDa	NDUFB6	**-2,05**
NADH dehydrogenase (ubiquinone) 1, subcomplex unknown, 2, 14.5kDa	NDUFC2	-1,56
Succinate dehydrogenase complex, subunit A, flavoprotein (Fp)	SDHA	-1,83
Ubiquinol-cytochrome c reductase, complex III subunit VII, 9.5kDa	UQCRQ	-1,65

Data report genes differentially modulated (above the cutoff of 1.5 fold of induction or below the cutoff of -1.5 fold of reduction) after DCA 30mM treatment in HL-60 cells. Genes significantly up-modulated (above the cutoff of 2 fold of induction) or down-modulated (below the cutoff of -2 fold of reduction) are indicated in boldface type.

As to regard the mitochondrial energy metabolism array data, DCA induced the down-modulation of two accessory subunits of the mitochondrial NADH dehydrogenase complex (NDUFA5 and NDUFB6) and of the succinate dehydrogenase complex subunit A (SDHA) genes, suggesting a slowing effect on the electrons' transfer along the mitochondrial membrane respiratory chain.

Table 9. Mitochondrial pathway activity signature genes expression in HL-60 cells after DCA treatment

Description	*Symbol*	*Fold Regulation*
Arrestin domain containing 3	ARRDC3	1,57
Ankyrin repeat and SOCS box containing 1	ASB1	nc
Cytochrome b-561 domain containing 1	CYB561D1	nc
DnaJ (Hsp40) homolog, subfamily B, member 1	DNAJB1	nc
Endothelin 1	EDN1	nc
Growth arrest and DNA-damage-inducible, beta	GADD45B	nc
Heat shock 70kDa protein 1A	HSPA1A	-1,94
Heat shock 70kDa protein 1B	HSPA1B	1,93
Low density lipoprotein receptor-related protein 5-like	LRP5L	nc
Polycistronic_H1_3	MitoH1	nc
Polycistronic_H2_200_12106_1	MitoH2_12106	nc
Polycistronic_H2_200_14573_3	MitoH2_14573	-1,51
Polycistronic_H2_200_4162_1	MitoH2_4162	-1,57
Polycistronic_H2_200_5726_3	MitoH2_5726	nc
RNU11	RNU11	nc
Solute carrier family 25 (mitochondrial phosphate carrier), member 25	SLC25A25	nc

Data presented in boldface type indicate genes significantly up-modulated (above the cutoff of 2 fold of induction) or down-modulated (below the cutoff of -2 fold of reduction). nc, not significant fold change in gene expression.

Mitochondrial dysfunction at transcriptional level can be reliably determined since the array includes 16 experimentally derived signature biomarker genes which, along with classification algorithms, are used to generate the activity score (Table 9). The calculation of this parameter did

not reveal any detectable change in mitochondrial pathway activity at gene expression level (pathway activity score upon DCA treatment = 0,062).

DCA induces the transcription of p21 in both p53$^{wild\text{-}type}$ and p53$^{mutated/null}$ leukemic cells

In the next set of experiments, we have investigated the mRNA levels of p21, whose *in vitro* induction represents a positive prognostic marker of response to therapy [**140**]. Surprisingly, DCA was equally effective in increasing the transcription levels of p21 in both primary p53$^{wild\text{-}type}$ and p53^{mutated} B-CLL leukemic cells (Figure 12A). The induction of p21 was confirmed at the protein level by Western blot analysis. Moreover, DCA significantly increased the steady-state mRNA levels in all the p53^{mutated} B cell lines (MAVER, MEC-1 and MEC-2) as well as in p53^{null} HL-60 (Figure 12A), thus confirming the ability of DCA to induce p21 expression independently of the presence of p53. In parallel, a confirmation of the lack of functional p53 transcriptional activity in both p53^{mutated} primary B-CLL cells and p53^{mutated} MAVER, MEC-1 and MEC-2 cell lines as well as in p53^{null} HL-60 was provided by the use of Nutlin-3. Indeed, while Nutlin-3 (10 μM) potently induced p21 transcription in primary p53$^{wild\text{-}type}$ B-CLL cells, it did not promote any modulation of p21 mRNA over the baseline in both primary p53^{mutated} B-CLL patient samples and p53$^{mutated/null}$ leukemic cell lines (Figure 12B), thus confirming the p53-independent activation of p21 by DCA in these cell models.

A

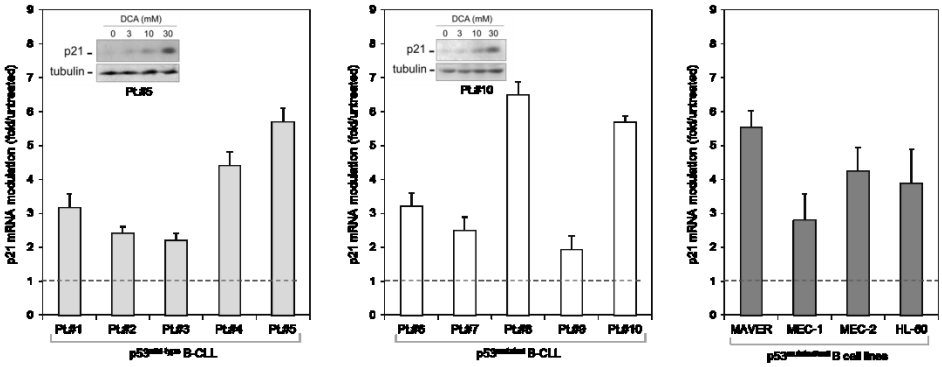

B

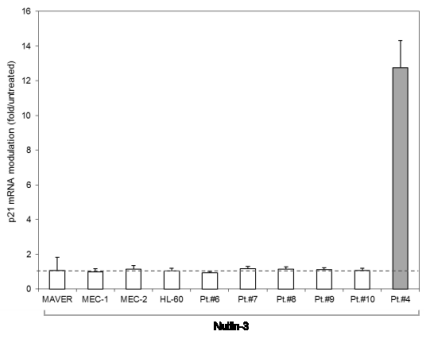

Figure 12. Induction of p21 by DCA in $p53^{mutated/null}$ leukemic cells. Levels of p21 were analyzed by quantitative RT-PCR in the $p53^{wilde\text{-}type}$ and $p53^{mutated}$ B-CLL patient samples, as well as in the $p53^{mutated}$ B leukemic cell lines (MAVER, MEC-1 and MEC-2) and in the $p53^{null}$ HL-60 cells. In A, levels of p21 modulation upon 24 hours of treatment with DCA (30 mM) are shown. Representative western blot results documenting induction of p21 protein by DCA in 2 B-CLL patient samples are shown in the insets. In B, the same cell cultures were exposed for 24 hours to Nutlin-3 (10 μM) before measurement of p21 levels. In parallel, as a positive control, p21 induction by Nutlin-3 was assessed in a $p53^{wild\text{-}type}$ B-CLL sample. In A and B, mRNA levels are expressed as fold of modulation with respect to the control untreated cultures set at 1. Results are reported as means±SD of at least three independent experiments, performed in duplicate, carried out on each leukemic sample.

DCA effects on HL-60 proteomic profile

To gain insight into the p53-independent induction of p21 by DCA, we adopted a proteomic approach using the HL-60 $p53^{null}$ leukemic model in order to rule out any potential interference by mutated p53 protein. For this purpose, we used a 1-DE gel approach for protein pre-fractionation integrated into a typical LC-MS/MS workflow for protein identification, performed as previously described [**142**]. A label-free approach (spectral counting) was then used for relative protein abundance quantification. Overall, our proteomic analysis identified 727 proteins in the total lysate of untreated and DCA treated HL-60 cells. According to statistical tests, HL-60 exposed to DCA 30mM for 24 hours exhibited a significant difference (at least 3-fold) in the abundance of 17 proteins compared to the untreated counterpart, with 10 up-regulated proteins and 7 down-regulated proteins (Tables 10 and 11).

Table 10. Differential expression data (as normalized spectral counts) for each identified protein whose abundance was significantly altered in HL-60 cells by DCA treatment

Protein name	*UniprotKB*	*HL-60 Untreated*						*HL-60 DCA30mM*						*Fold regulation*[g]
		1R[a] *NSC*[d]	*2R*[b] *NSC*[d]	*3R*[c] *NSC*[d]	*Average NSC*	*SD*[e]	*%CV*[f]	*1R*[a] *NSC*[d]	*2R*[b] *NSC*[d]	*3R*[c] *NSC*[d]	*Average NSC*	*SD*[e]	*%CV*[f]	
ADP/ATP translocase 2 (ANT2)	P05141	26	35	37	32.67	5.86	17.94	1	1	1	1.00	0.00	0.00	-32.67
ADP-ribosylation factor 4	P18085	1	1	1	1.00	0.00	0.00	6	6	5	5.67	0.58	10.19	5.67
ADP-ribosylation factor 5	P84085	1	1	1	1.00	0.00	0.00	8	8	6	7.33	1.15	15.75	7.33
Asparagine-tRNA ligase, cytoplasmic	O43776	4	4	5	4.33	0.58	13.32	17	20	21	19.33	2.08	10.77	4.46
Endoplasmic reticulum resident protein 44	Q9BS26	9	7	7	7.67	1.15	15.06	2	1	3	2.00	1.00	50.00	-3.83
Eukaryotic translation initiation factor 2 subunit 3	P41091	3	2	2	2.33	0.58	24.74	5	9	9	7.67	2.31	30.12	3.29
Glycine-tRNA ligase	P41250	1	1	1	1.00	0.00	0.00	9	10	11	10.00	1.00	10.00	10.00
Growth factor receptor-bound protein 2	P62993	7	6	7	6.67	0.58	8.66	1	1	1	1.00	0.00	0.00	-6.67
Histidine--tRNA ligase, cytoplasmic	P12081	5	6	8	6.33	1.53	24.12	1	1	1	1.00	0.00	0.00	-6.33
Histone H3.1	P68431	1	1	1	1.00	0.00	0.00	8	7	4	6.33	2.08	32.87	6.33
Histone H3.2	Q71DI3	1	1	1	1.00	0.00	0.00	8	5	5	6.00	1.73	28.87	6.00
Interleukin enhancer-binding factor 3	Q12906	1	3	1	1.67	1.15	69.28	11	7	5	7.67	3.06	39.85	4.60
NAD(P) transhydrogenase, mitochondrial (NNT)	Q13423	1	1	1	1.00	0.00	0.00	5	9	8	7.33	2.08	28.39	7.33
Prothymosin alpha	P06454	1	1	1	1.00	0.00	0.00	8	17	17	14.00	5.20	37.12	14.00
Ribonucleoside-diphosphate reductase large subunit	P23921	9	13	11	11.00	2.00	18.18	4	4	3	3.67	0.58	15.75	-3.00
Serine/threonine-protein phosphatase PP1-alpha catalytic subunit	P62136	14	12	12	12.67	1.15	9.12	9	1	1	3.67	4.62	125.97	-3.45
Tubulin-tyrosine ligase-like protein 12	Q14166	9	10	8	9.00	1.00	11.11	2	4	3	3.00	1.00	33.33	-3.00

[a],first replicate; [b],second replicate; [c],third replicate; [d],number of normalized spectral counts (NSC); [e],standard deviation of the averaged NSC; [f],coefficient of variation (CV%); [g],fold regulation in expression HL60 DCA treated cells vs non-treated cells.

Table 11. Proteins significantly altered (OPLS-DA, Mann-Whitney, p<0,05) in HL-60 cells after DCA treatment

Description	*Accession Number*	*UniProtkB*	*Fold regulation*
ADP/ATP translocase 2 (ANT2)	ADT2_HUMAN	P05141	-32.67
ADP-ribosylation factor 4	ARF4_HUMAN	P18085	5.67
ADP-ribosylation factor 5	ARF5_HUMAN	P84085	7.33
Asparagine-tRNA ligase, cytoplasmic	SYNC_HUMAN	O43776	4.46
Endoplasmic reticulum resident protein 44	ERP44_HUMAN	Q9BS26	-3.83
Eukaryotic translation initiation factor 2 subunit 3	IF2G_HUMAN	P41091	3.29
Glycine-tRNA ligase	SYG_HUMAN	P41250	10.00
Growth factor receptor-bound protein 2	GRB2_HUMAN	P62993	-6.67
Histidine-tRNA ligase, cytoplasmic	SYHC_HUMAN	P12081	-6.33
Histone H3.1	H31_HUMAN	P68431	6.33
Histone H3.2	H32_HUMAN	Q71DI3	6.00
Interleukin enhancer-binding factor 3	ILF3_HUMAN	Q12906	4.60
NAD(P) transhydrogenase, mitochondrial (NNT)	NNTM_HUMAN	Q13423	7.33
Prothymosin alpha	PTMA_HUMAN	P06454	14.00
Ribonucleoside-diphosphate reductase large subunit	RIR1_HUMAN	P23921	-3.00
Serine/threonine-protein phosphatase PP1-alpha catalytic subunit	PP1A_HUMAN	P62136	-3.45
Tubulin-tyrosine ligase-like protein 12	TTL12_HUMAN	Q14166	-3.00

Data report proteins differentially modulated (above the cutoff of 3 fold of induction or below the cutoff of -3 fold of reduction) after DCA 30mM treatment in HL-60 cells.

Network analysis, using MetaCore bioinformatic tools of the 17 significantly deregulated proteins, revealed the involvement of *Cellular metabolic processes* as the main GO processes altered by DCA treatment (Figure 13A). In addition, when MetaCore software was used to map the shortest paths of interactions among the differentially expressed proteins, 12 out of 17 proteins were brought together with p21 as the hub of the identified network (Figure 13B). Among the significantly deregulated proteins there was a relevant modulation of two mitochondrial proteins, i.e. the down-regulation of ANT2 (ADP/ATP translocase 2), a bi-functional protein that mediates the vital exchange of cytosolic ADP and mitochondrial ATP and participates to mitochondrial membrane permeability transition pore [**143**] and the up-regulation of NNT (NAD(P) transhydrogenase, mitochondrial), an integral protein located in the inner mitochondrial membrane that contributes to an elevated mitochondrial NADPH/NADP(+) ratio.

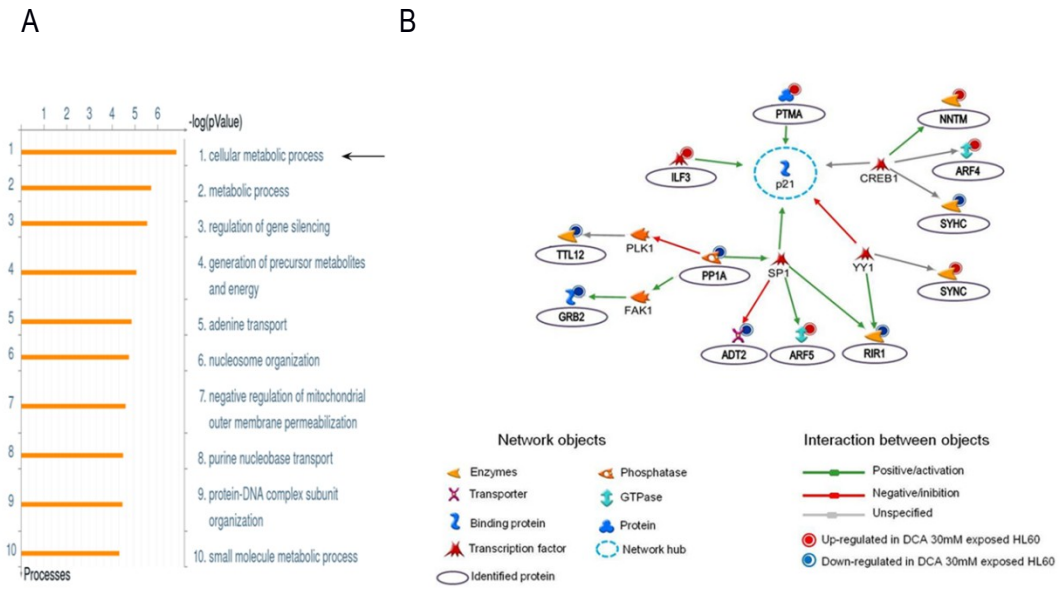

Figure 13. Role of p21 in mediating the anti-leukemic activity of DCA in $p53^{null}$ leukemic cells. In A-B, proteomic profiling in HL-60 cells upon DCA treatment revealed significant different (at least 3 folds) levels for 17 proteins in DCA treated cultures compared to the untreated cells (Table 11). In A, the top ten GO processes, prioritized in according to p-value, in response to DCA treatment is shown. In B, the protein network generated by the shortest path algorithm using the list of the differently expressed proteins (more than 3 fold induction/reduction) is reported. Nodes represent proteins and the different shapes of the nodes represent the functional class of the proteins. Circles evidence protein identified in our proteomic analysis. Lines connecting the nodes indicate indirect interactions (activation, induction, modification) or direct binding; the arrowheads indicate the direction of the interaction. Blue broken line circles highlight network hubs as indicated by network statistics.

Interestingly p21 was directly connected with interleukin enhancer-binding factor 3 (ILF3, also known as NFAT-90 or NF90), a regulator of p21 at transcriptional and post-transcriptional levels [**144,145**] (Figure 14) and prothymosin alpha (PTMA), that exerted a broader effect on transcription, due to its ability to interact with histones and affect chromatin remodeling processes [**146**].

Numerous reports document the direct interaction of the heterodimeric nuclear factor 90/ nuclear factor 45 complex (ILF3/ILF2) with DNA, acting as regulator of gene expression at transcriptional level; indeed this complex has been shown to regulate the activity of several cellular promoters through direct interaction with a specific target DNA sequence, the purine-rich antigen receptor response element/nuclear factor of activated T-cells (NF-AT) binding site (ARRE)/NF-AT [**144**]. The same recognition motif has been predicted to be present in the regulatory region of the p21/CDKN1A gene through bioinformatics tool (MatInspector analyses of Genomatix), with significantly high similarity score. Nevertheless, in addition to the above described role in transcriptional control, it is documented that NF45 and NF90 also interact with RNA, acting at

multiple levels: indeed NF90 regulates the post-transcriptional stabilization of RNA molecules, nuclear export to cytoplasm, RNA splicing and translation [**144**]. In particular, the 3'-UTR of both the human and murine p21 mRNA is predicted to adopt secondary structures that includes regions of double-stranded RNA and hairpin-loops with AU-rich elements which represent binding targets for NF90. Gene-targeted NF90(-/-) mice, completely lacking NF90 protein, demonstrate severely reduced expression of p21, both at mRNA and at protein level, compared to wild-type and heterozygote littermates, leading to the conclusion that NF90 is a critical determinant of post-transcriptional stabilization of p21 mRNA, stabilizing the mRNA against rapid degradation, and consequently contributing to the up-regulation of p21 gene expression [**145**].

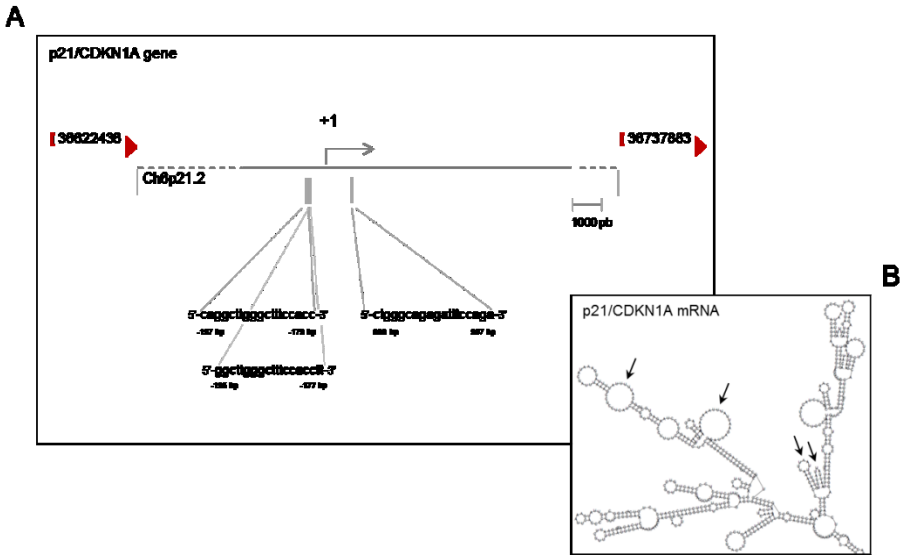

Figure 14. Mechanisms of p21/CDKN1A gene regulation by ILF3. Schematic representation of the predicted ILF3 binding sites on the regulatory region of the human p21/CDKN1A gene (A) and on the p21 mRNA 3'-UTR secondary structure (B), supporting the transcriptional and post-transcriptional regulation of p21/CDKN1A by ILF3. In A, the purine-rich NF-AT/ILF3 binding sites, predicted by computational analysis (MatInspector analyses of Genomatix), are evidenced in the regulatory region of the human p21/CDKN1A gene. In B, mRNA 3'-UTR secondary structure analysis (RNA fold program from the Vienna RNA Package, used to perform the secondary structure predictions and folding calculations) of a partial region of p21/CDKN1A is represented; arrows indicate the AU-rich elements in the sequence recognized by ILF3, involved in the stabilization of p21 mRNA.

Role of ILF3-p21 axis in DCA induced cytotoxicity

On the base of the proteomic results, we next tested the potential role of p21 in mediating the anti-leukemic activity of DCA using again the $p53^{null}$ HL-60 cells as model system, by utilizing siRNAs to attenuate p21 expression. As shown in Figure 15A, once confirmed the effective knock-

down of p21 expression through quantitative RT-PCR both at baseline and after DCA treatment, we observed a significant ($p<0.05$) reduction in DCA-induced cytotoxicity in p21 siRNA transfected cells with respect to cells transfected with a scrambled control siRNA. This set of data confirmed that p21 plays a central role in mediating cytotoxicity of DCA not only in $p53^{wild\text{-}type}$ B leukemic cells but also in $p53^{deficient}$ leukemic cells.

Subsequently, in order to disclose the mechanism of p21 regulation by DCA, we attenuate ILF3 expression. As shown in Figure 13B, the knock-down of ILF3 expression by siRNA transfection determined the concomitant reduction in p21 mRNA levels both in untreated culture and upon DCA exposure, consistently with the documented role of ILF3 as a regulator of p21 at transcriptional and post-transcriptional levels. The involvement of ILF3 in DCA anti-leukemic signaling pathway, in absence of functional p53 pathway, was revealed by the effect of its down-modulation in attenuating DCA cytotoxicity, similarly to the effect resulted by p21 gene silencing (Figure 15B-C).

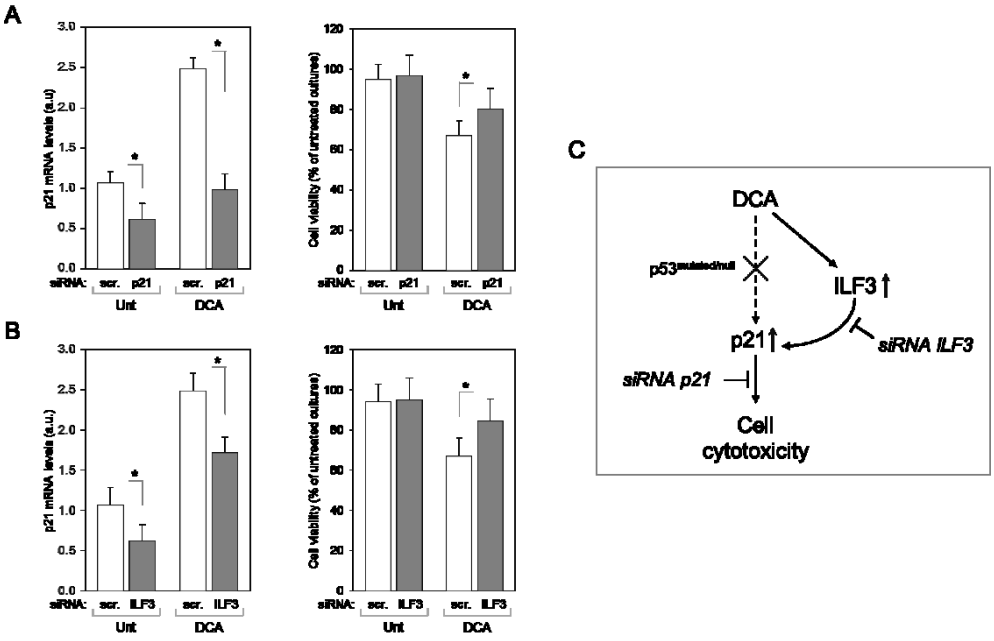

Figure 15. Role of p21 and ILF3 pathway in mediating the anti-leukemic activity of DCA in $p53^{null}$ leukemic cells. In A-B, HL-60 cells were transfected with either control scrambled (scr) siRNA, or p21 siRNA (A) or ILF3 siRNA (B) before treatment with DCA (30 mM). After transfection, levels of p21 mRNA were analyzed by quantitative RT-PCR (A-B). Data are expressed as arbitrary units (a.u.). In parallel transfected cultures were analyzed for cell viability upon exposure to DCA; results are expressed as percentage of viable cells with respect to the control cultures (set to 100%). Data are reported as means±SD of results from three independent experiments, each performed in duplicate (Mann-Whitney rank-sum test; asterisk, $p<0.05$). In C, a schematic representation of the potential p53-independent pathway mediating the anti-leukemic activity of DCA is shown.

On the other hand, knock-down of ILF3 expression in p53$^{wilde\text{-}type}$ cells did not determine significant modulatory effects on p21 (both in untreated culture and upon DCA exposure; Figure 16). Although this is not a direct evidence of the role of p53 in p21 regulation, nevertheless it suggests a prominent role of p53-pathway in the p21 induction by DCA in p53$^{wild\text{-}type}$ cells.

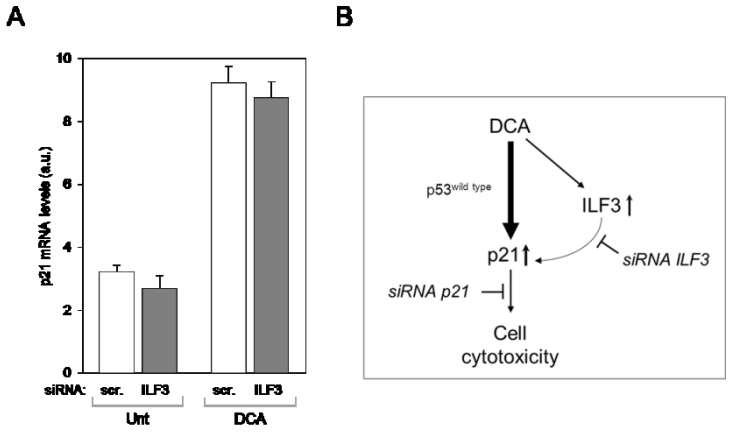

Figure 16. Analysis of the DCA-ILF3-p21 axis in p53$^{wild\text{-}type}$ leukemic cells. In A, p53$^{wild\text{-}type}$ JVM-2 cells were transfected with either control scrambled (scr) siRNA or ILF3 siRNA, before treatment with DCA (30 mM). Upon ILF3 silencing, levels of p21 mRNA were assessed by quantitative RT-PCR, both in untreated and DCA treated cells. Data are expressed as arbitrary units (a.u.) and reported as means±SD of results from three independent experiments, each performed in duplicate. In B, a schematic representation of the hypothetic p53-dependent and p53-independent pathways mediating the p21 modulation in response to DCA.

Discussion

Recently it has been proposed that the metabolic phenotype in cancer is to be ascribed to a potentially plastic mitochondrial remodeling that results in the inhibition of oxidative phosphorylation, improvement in glycolysis and reduction in apoptosis level. Cancer associated oxidative stress and aerobic glycolysis have been documented to be active also in hematological malignancies, including B-CLL [**85**], with the prevalence of oxidative stress, adaptation to permanent intrinsic oxidative stress and mitochondrial biogenesis [**82**]. Thus, agents directed against these unique metabolic features of cancer cells might represent an opportunity to improve current treatments, in particular with the aim of overcoming drug resistance in leukemic cells.

In this study, we have demonstrated for the first time that the mitochondria-targeting small molecule DCA exerts cytotoxic activity *in vitro* at comparable levels in both primary $p53^{wild\text{-}type}$ and $p53^{mutated}$ B-CLL patient cells, as well as in $p53^{wild\text{-}type}$ and in $p53^{mutated/null}$ leukemic cell lines, in a range of concentrations previously used by other authors in *in vitro* models of solid tumors [**101-103,105**]. On the other hand, DCA marginally affected cell viability of primary normal peripheral blood mononuclear cells obtained from healthy individuals. These findings are particularly remarkable since patients harboring TP53 mutations have a poor prognosis and still limited therapeutic options [**31**]. Indeed, p53 mutations are known to interfere with the normal response of human cells to oxidative stress. The failure of p53 mutant-expressing cells to restore a reducing oxidative environment is often accompanied by increased survival [**147**], which represents an aspect of the gain of function of the pro-oncogenic activity of mutated TP53. In considering the potential relevance of our *in vitro* studies, suggesting the therapeutic use of DCA as anti-leukemic molecule, it should be underlined that there are 40 years of human experience in the treatment of lactic acidosis and inherited mitochondrial diseases, with mechanistic studies of DCA in human tissues after oral use, pharmacokinetic and toxicity data from randomized studies [**148**]. Moreover, preclinical studies demonstrated the DCA efficacy against solid tumors, as well as on multiple myeloma, and confirmed a relatively low toxicity of this molecule with good tolerability and low incidence of adverse effects. In fact, DCA is currently being included in phase I/II clinical trials for glioblastoma, gliomas and other

solid tumors [**106**]. These data support an easy translation of DCA in clinical settings. An additional interesting characteristic of this molecule is its low cost.

At molecular level, by using as a model system a set of B leukemic cell lines, we have demonstrated that DCA induces both cell cycle arrest in the G1 phase, senescence and apoptosis through both p53-dependent and p53-independent pathways. In the first part of our study, focused on p53 wild-type B-CLL (which represent the great majority), our investigations revealed that DCA induced post-transcriptional modifications of p53 with activation of the p53 transcriptional activity, as documented by the induction of several canonical p53 target genes, such as MDM2, p21 and PUMA. Another interesting finding was the ability of DCA to potently synergize with Nutlin-3, a non-genotoxic activator of the p53 pathway, in promoting cytotoxicity in B leukemic cell lines as well as in primary B-CLL patient cells, with significantly less toxicity on normal PBMC. Although the contribution of the transcriptional activity of p53 in promoting leukemic cytotoxicity is still under debate, as transcriptional independent activities have also been demonstrated in previous studies performed with Nutlin-3 [**29,30**], our data demonstrated the existence of a correlation between the ability to promote the transcription of p53 transcriptional targets, and in particular p21, and the synergistic cytotoxic activity in response to the DCA+Nutlin-3 treatment. Interestingly, while the DCA+Nutlin-3 combination was extremely efficient in inducing the transcription of p21 in both primary B-CLL patient samples and B leukemic cell lines, it was significantly less efficient when added to primary normal PBMC. The demonstration that DCA+Nutlin-3 potently synergized in inducing the transcriptional activation of p21 is noteworthy since the transcriptional induction of p21 has been involved in mediating the therapeutic effect of chemotherapeutic drugs in B-CLL [**140**].

As anticipated above, DCA exhibits anti-leukemic activity also independently of p53 functionality. DCA efficiently induced mitochondrial damage, documented by morphological remodeling of mitochondrial structure, mitochondrial depolarization and reduction in ATP synthesis, in all leukemic cell lines investigated independently by the p53 status. Proteomic analyses in p53 null leukemic cells revealed a relevant modulation of proteins involved in the metabolic processes including proteins of the mitochondrial inner membrane, i.e. the down-regulation of adenine nucleotide translocase 2 (ANT2) and the up-regulation of nicotinamide nucleotide transhydrogenase (NNT). ANT2 exerts a crucial role in the metabolic adaptation of cancer cells, contributing to the maintenance of the mitochondrial membrane potential ($\Delta\Psi m$) under glycolytic conditions, ensuring cell survival upon oxidative phosphorylation impairment and preventing apoptotic cell death [**149**]. NNT contributes to an elevated mitochondrial NADPH/NADP(+) ratio, participating in the defence against mitochondrial oxidative stress [**150**].

In parallel, we documented that DCA induced the transcription of p21 through the induction of the transcription factor ILF3 in a p53-independent manner.

Recent studies confirmed that p21 is necessary for the induction of mitochondrial dysfunction observed in senescence and this event maintains a constant DNA damage response leading to prolonged cell cycle arrest [**151**]. P21 prevents cancer cell growth due to its ability to transiently or permanently stop proliferation, thus being an important component of tumor suppressor mechanisms. Indeed, it has recently been demonstrated that p21 can be down-regulated by several microRNA expressed in cancer cells [**152,153**]. Concurrently, although p21 levels have been found elevated in some cancers without signs of growth inhibition [**154**] and in some experimental settings it has been proposed that p21 can actually favor transformation by inhibiting apoptosis [**153**], other studies have recently shown that p21 can also trigger cell death [**140,151**]. At present, it is not well understood how p21 exerts these radically different functions or even if they reside in separate domains of the protein.

Conclusions

In spite of the discrepancies present in the scientific literature, overall our data clearly point to the tumor-suppressor activity of p21 in the context of DCA-induced cytotoxicity on both $p53^{wilde\text{-}type}$ as well as on $p53^{mutated/null}$ B-leukemic cell lines, in agreement with the demonstration that the *in vitro* activation of p21 in B-CLL accurately predicts the therapeutic response *in vivo* of B-CLL [**140**].

Since p53 mutations still represent one of the major negative prognosticators of B-CLL, we believe that the therapeutic potential of DCA should be further evaluated possibly in combination with other innovative anti-leukemic drugs.

References

1. Oscier D, Dearden C, Eren E, et al. Guidelines on the diagnosis and management of chronic lymphocytic leukemia. Br J Haematol. 2012 Dec;159(5):541-564.
2. Zenz T, Mertens D, Kuppers R, et al. From pathogenesis to treatment of chronic lymphocytic leukemia. Nat Rev Cancer 2010; 10: 37–50.
3. Puente XS, Pinyol M, Quesada V, et al. Whole-genome sequencing identifies recurrent mutations in chronic lymphocytic leukemia. Nature. 2011;475(7354):101-105.
4. Quesada V, Conde L, Villamor N, et al. Exome sequencing identifies recurrent mutations of the splicing factor SF3B1 gene in chronic lymphocytic leukemia. Nat Genet 2011, 44:47–52.
5. Wang L, Lawrence MS, Wan Y, et al. SF3B1 and other novel cancer genes in chronic lymphocytic leukemia. N Engl J Med. 2011;365:2497-2506.
6. Zhang J, Xiang Y, Ding L, et al. Using gene co-expression network analysis to predict biomarkers for chronic lymphocytic leukemia. BMC Bioinformatics. 2010 Oct 28;11 Suppl 9:S5.
7. Orchard JA, Ibbotson RE, Davis Z, et al. ZAP-70 expression and prognosis in chronic lymphocytic leukemia. Lancet 2004; 363:105-111.
8. Damle RN, Temburni S, Calissano C, et al. CD38 expression labels an activated subset within chronic lymphocytic leukemia clones enriched in proliferating B cells. Blood 2007;110:3352–3359.
9. Quesada V, Ramsay AJ, Rodríguez D, et al. The genomic landscape of chronic lymphocytic leukemia: clinical implications. BMC Med. 2013 May 9;11:124.
10. Haslinger C, Schweifer N, Stilgenbauer S, et al. Microarray gene expression profiling of B-cell chronic lymphocytic leukemia subgroups defined by genomic aberrations and VH mutation status. J Clin Oncol 2004;22:3937-3949.
11. Hamblin TJ, Davis Z, Gardiner A, et al: Unmutated Ig V (H) genes are associated with a more aggressive form of chronic lymphocytic leukemia. Blood 1999;94:1848–1854.
12. Tobin G, Thunberg U, Johnson A, et al. Chronic lymphocytic leukemias utilizing the VH3-21 gene display highly restricted Vlambda2-14 gene use and homologous CDR3s: implicating recognition of a common antigen epitope. Blood 2003;101:4952-4957.
13. Ouillette P, Collins R, Shakhan S, et al. Acquired genomic copy number aberrations and survival in chronic lymphocytic leukemia. Blood 2011; 118:3051–3061.
14. Calin GA, Dumitru CD, Shimizu M, et al. Frequent deletions and down-regulation of micro- RNA genes miR15 and miR16 at 13q14 in chronic lymphocytic leukemia. Proc Natl Acad Sci USA. 2002;99:15524–15529.

15. Döhner H, Stilgenbauer S, Benner A, et al. Genomic aberrations and survival in chronic lymphocytic leukemia. N Engl J Med 2000;343:1910–1916.
16. Arruga F, Gizdic B, Serra S, et al. Functional impact of NOTCH1 mutations in chronic lymphocytic leukemia. Leukemia. 2014;28(5):1060-1070.
17. Landau DA, Carter SL, Stojanov P, et al. Evolution and impact of subclonal mutations in chronic lymphocytic leukemia. Cell 2013;152: 714–726.
18. Landau DA, Wu CJ. Chronic lymphocytic leukemia: molecular heterogeneity revealed by high-throughput genomics. Genome Med 2013; 5: 47.
19. Ramsay AJ, Martinez-Trillos A, Jares P, et al. Next-generation sequencing reveals the secrets of the chronic lymphocytic leukemia genome. Clin Transl Oncol 2013, 15:3–8.
20. Austen B, Powell JE, Alvi A, et al. Mutations in the ATM gene lead to impaired overall and treatment-free survival that is independent of IGVH mutation status in patients with B-CLL. Blood. 2005; 106:3175–3182.
21. Zenz T, Eichhorst B, Busch R, et al. TP53 mutation and survival in chronic lymphocytic leukemia. J Clin Oncol. 2010; 28:4473–4479.
22. Trbusek M, Smardova J, Malcikova J, et al. Missense mutations located in structural p53 DNA binding motifs are associated with extremely poor survival in chronic lymphocytic leukemia. JClin Oncol. 2011; 29:2703–2708.
23. Fabbri G, Rasi S, Rossi D, et al. Analysis of the chronic lymphocytic leukemia coding genome: role of NOTCH1 mutational activation. J Exp Med 2011; 208: 1389–1401.
24. Ngo VN, Young RM, Schmitz R, et al. Oncogenically active MYD88 mutations in human lymphoma. Nature. 2011; 470:115–119.
25. Zenz T, Vollmer D, Trbusek M, et al. TP53 mutation profile in chronic lymphocytic leukemia: Evidence for a disease specific profile from a comprehensive analysis of 268 mutations. Leukemia 2010;24:2072-2079.
26. Zenz T, Häbe S, Denzel T, et al. Detailed analysis of p53 pathway defects in fludarabine-refractory chronic lymphocytic leukemia (CLL): dissecting the contribution of 17p deletion, TP53 mutation, p53-p21 dysfunction, and miR34a in a prospective clinical trial. Blood. 2009;114(13):2589-2597.
27. Rossi D, Fangazio M, Rasi S, et al: Disruption of BIRC3 associates with fludarabine chemorefractoriness in TP53 wild-type chronic lymphocytic leukemia. Blood 2012;119:2854–2862.
28. Gonzalez D, Martinez P, Wade R, et al. Mutational status of the TP53 gene as a predictor of response and survival in patients with chronic lymphocytic leukemia: results from the LRF CLL4 trial. J Clin Oncol 2011;29:2223–2229.
29. Secchiero P, di Iasio MG, Gonelli A, et al. The MDM2 inhibitors Nutlins as an innovative therapeutic tool for the treatment of hematological malignancies. Curr Pharm Des. 2008;14:2100-2110.
30. Secchiero P, Zauli G. TNF-related apoptosis-inducing ligand and the regulation of hematopoiesis. Curr Opin Hematol. 2008;15:42-48.

31. Rossi D, Khiabanian H, Spina V, et al. Clinical impact of small TP53 mutated subclones in chronic lymphocytic leukemia. Blood. 2014; 123: 2139-2147.
32. Zent CS, Taylor RP, Lindorfer MA, et al. Chemoimmunotherapy for relapsed/refractory and progressive 17p13 deleted chronic lymphocytic leukemia (CLL) combining pentostatin, alemtuzumab, and low dose rituximab is effective and tolerable and limits loss of CD20 expression by circulating CLL cells. Am J Hematol. 2014; 89: 757-765.
33. Stankovic T, Hubank M, Cronin D, et al. Microarray analysis reveals that TP53- and ATM-mutant B-CLLs share a defect in activating proapoptotic responses after DNA damage but are distinguished by major differences in activating prosurvival responses. Blood. 2004;103:291-300.
34. O'Neill LA, Bowie AG. The family of five: TIR-domain-containing adaptors in Toll-like receptor signalling. Nature Rev. Immunol. 2007;7:353–364.
35. Burger JA, Quiroga MP, Hartmann E, et al. High-level expression of the T-cell chemokines CCL3 and CCL4 by chronic lymphocytic leukemia B cells in nurselike cell cocultures and after BCR stimulation. Blood. 2009;113:3050–3058.
36. Muzio M, Scielzo C, Bertilaccio MT, et al. Expression and function of toll like receptors in chronic lymphocytic leukemia cells. Br. J. Haematol. 2009; 144:507–516.
37. Rosati E, Sabatini R, Rampino G, et al. Constitutively activated Notch signaling is involved in survival and apoptosis resistance of B-CLL cells. Blood 2009; 113: 856–865.
38. Villamor N, Conde L, Martínez-Trillos A, et al. NOTCH1 mutations identify a genetic subgroup of chronic lymphocytic leukemia patients with high risk of transformation and poor outcome. Leukemia 2013; 27: 1100–1106.
39. Oscier DG, Rose-Zerilli MJ, Winkelmann N, et al. The clinical significance of NOTCH1 and SF3B1 mutations in the UK LRF CLL4 trial. Blood 2013;121:468–475.
40. Rossi D, Bruscaggin A, Spina V, et al. Mutations of the SF3B1 splicing factor in chronic lymphocytic leukemia: association with progression and fludarabine-refractoriness. Blood. 2011;118(26): 6904-6908.
41. Schnaiter A, Paschka P, Rossi M, et al. NOTCH1, SF3B1, and TP53 mutations in fludarabinerefractory CLL patients treated with alemtuzumab: results from the CLL2H trial of the GCLLSG. Blood. 2013;122(7):1266-1270.
42. Messina M, Del Giudice I, Khiabanian H, et al. Genetic lesions associated with chronic lymphocytic leukemia chemo-refractoriness. Blood. 2014 Apr 10;123(15):2378-88.
43. Hallek M, Fischer K, Fingerle-Rowson G, et al; International Group of Investigators; German Chronic Lymphocytic Leukemia Study Group. Addition of rituximab to fludarabine and cyclophosphamide in patients with chronic lymphocytic leukemia: a randomised, open-label, phase 3 trial. Lancet. 2010;376(9747):1164-1174.
44. Zenz T, Gribben JG, Hallek M, et al. Risk categories and refractory CLL in the era of chemoimmunotherapy. Blood. 2012;119(18): 4101-4107.
45. Oscier DG, Rose-Zerilli MJ, Winkelmann N, et al: The clinical significance of NOTCH1 and SF3B1

mutations in the UK LRF CLL4 trial. Blood 2013, 121:468–475.

46. Mansouri L, Cahill N, Gunnarsson R, et al. NOTCH1 and SF3B1 mutations can be added to the hierarchical prognostic classification in chronic lymphocytic leukemia. Leukemia 2012; 27:512–514.
47. Puente XS, Lopez-Otin C. The evolutionary biography of chronic lymphocytic leukemia. Nat Genet 2013;45:229–231.
48. CLL trialists collaborative group. Chemotherapeutic options in chronic lymphocytic leukemia. J Natl Cancer Inst. 1999;91:861-868.
49. Hallek M. Signaling the end of chronic lymphocytic leukemia: new frontline treatment strategies. Blood. 2013 Nov 28;122(23):3723-34.
50. Rai KR, Peterson BL, Appelbaum FR, et al. Fludarabine compared with chlorambucil as primary therapy for chronic lymphocytic leukemia. N Engl J Med. 2000;343(24): 1750-1757.
51. Hallek M, Eichhorst BF. Chemotherapy combination treatment regimens with fludarabine in chronic lymphocytic leukemia. Hematol J. 2004;5(Suppl 1):S20-S30.
52. Eichhorst BF, Busch R, Hopfinger G, et al. Fludarabine plus cyclophosphamide versus fludarabine alone in first line therapy of younger patients with chronic lymphocytic leukemia. Blood. 2006;107:885-891.
53. Flinn IW, Neuberg DS, Grever MR, et al. Phase III trial of fludarabine plus cyclophosphamide compared with fludarabine for patients with previously untreated chronic lymphocytic leukemia: US Intergroup Trial E2997. J Clin Oncol. 2007;25(7):793-798.
54. Catovsky D, Richards S, Matutes E, et al. Assessment of fludarabine plus cyclophosphamide for patients with chronic lymphocytic leukaemia (the LRF CLL4 Trial): a randomised controlled trial. Lancet. 2007;370(9583):230-239.
55. Schulz H, Bohlius JF, Trelle S, et al. Immunochemotherapy with rituximab and overall survival in patients with indolent or mantle cell lymphoma: a systematic review and meta-analysis. J Natl. Cancer Inst 2007;99:706-714.
56. Huhn D, von Schilling C, Wilhelm M, et al. Rituximab therapy of patients with B-cell chronic lymphocytic leukemia. Blood 2001;98:1326–1331.
57. Keating MJ, O'Brien S, Albitar M, et al. Early results of a chemoimmunotherapy regimen of fludarabine, cyclophosphamide, and rituximab as initial therapy for chronic lymphocytic leukemia. J Clin Oncol 2005;23:4079–4088.
58. Tam CS, O'Brien S, Wierda W, et al. Long-term results of the fl udarabine, cyclophosphamide, and rituximab regimen as initial therapy of chronic lymphocytic leukemia. Blood 2008;112:975–980.
59. Wierda WG, Kipps TJ, Mayer J, et al. Ofatumumab as single-agent CD20 immunotherapy in fludarabine-refractory chronic lymphocytic leukemia. J Clin Oncol. 2010;28(10): 1749-1755.
60. Lozanski G, Heerema NA, Flinn IW, et al. Alemtuzumab is an effective therapy for chronic lymphocytic leukemia with p53 mutations and deletions. Blood. 2004;103(9):3278-3281.
61. Wiestner A. Emerging role of kinase-targeted strategies in chronic lymphocytic leukemia. Hematology Am Soc Hematol Educ Program. 2012;2012:88-96.

62. Isfort S, Cramer P, Hallek M. Novel and emerging drugs for chronic lymphocytic leukemia. Curr Cancer Drug Targets. 2012;12(5):471-483.
63. Stevenson FK, Krysov S, Davies AJ, et al. B-cell receptor signaling in chronic lymphocytic leukemia. Blood. 2011;118(16):4313-4320.
64. Hoellenriegel J, Meadows SA, Sivina M, et al. The phosphoinositide 39-kinase delta inhibitor, CAL-101, inhibits B-cell receptor signaling and chemokine networks in chronic lymphocytic leukemia. Blood. 2011;118(13):3603-3612.
65. Brown JR, Furman RR, Flinn IW, et al. Final results of a phase 1 study of idelalisib (GS-1101) a selective inhibitor of phosphatidylinositol 3-kinase p110 delta (PI3Kdelta) in patients with relapsed or refractory CLL. J Clin Oncol. 2013; 31(Suppl):7003.
66. Herman SE, Gordon AL, Hertlein E, et al. Bruton tyrosine kinase represents a promising therapeutic target for treatment of chronic lymphocytic leukemia and is effectively targeted by PCI-32765. Blood. 2011;117(23):6287-6296.
67. Advani RH, Buggy JJ, Sharman JP, et al. Bruton tyrosine kinase inhibitor ibrutinib (PCI-32765) has significant activity in patients with relapsed/ refractory B-cell malignancies. J Clin Oncol. 2013;31(1):88-94.
68. Byrd JC, Furman RR, Coutre SE, et al. Targeting BTK with ibrutinib in relapsed chronic lymphocytic leukemia. N Engl J Med. 2013;369(1):32-42.
69. Cairns RA, Harris IS, Mak TW. Regulation of cancer cell metabolism. Nature Rev Cancer 2011;11, 85-95.
70. Parsons DW, Jones S, Zhang X, et al. An integrated genomic analysis of human glioblastoma multiforme. Science. 2008; 321, 1807–1812.
71. Stratton MR, Campbell P J, Futreal P A. The cancer genome. Nature 2009;458, 719–724.
72. DeBerardinis RJ, Thompson CB. Cellular metabolism and disease: what do metabolic outliers teach us? Cell. 2012;148, 1132–1144.
73. Hsu PP, Sabatini DM. Cancer cell metabolism: Warburg and beyond. Cell. 2008;134, 703–707.
74. Tennant DA, Durán RV, Boulanbel H. et al. Metabolic transformation in cancer. Carcinogenesis. 2009;30, 1269–1280.
75. Kim JW, Dang CV. Cancer's molecular sweet tooth and the Warburg effect. Cancer Res. 2006;66:8927–30.
76. Bonnet S, Archer SL, Allalunis-Turner J, et al. A mitochondrialK+ channel axis is suppressed in cancer and its normalization promotes apoptosis and inhibits cancer cell growth. Cancer Cell. 2007;11, 37–51.
77. Semenza GL, Artemov D, Bedi A, et al 'The metabolism of tumours': 70 years later. Novartis Found. Symp. 2001;240, 251–260; discussion 260–254.
78. Vousden KH, Ryan KM. p53 and metabolism. Nat Rev Cancer. 2009;9(10):691-700.
79. Stockwin LH, Yu SX, Borgel S, et al. Sodium dichloroacetate selectively targets cells with defects in the mitochondrial ETC. Int J Cancer. 2010;127(11):2510-2519.

80. Chen Z, Lu W, Garcia-Prieto C, et al. The Warburg effect and its cancer therapeutic implications. J Bioenerg Biomembr 2007;39:267–74.
81. Cairns R, Papandreou I, Denko N. Overcoming physiologic barriers to cancer treatment by molecularly targeting the tumor microenvironment. Mol. Cancer Res. 2006;4, 61–70.
82. Jitschin R, Hofmann AD, Bruns H, et al. Mitochondrial metabolism contributes to oxidative stress and reveals therapeutic targets in chronic lymphocytic leukemia. Blood. 2014;123:2663-2672.
83. Samudio I, Fiegl M, Andreeff M. Mitochondrial uncoupling and the Warburg effect: molecular basis for the reprogramming of cancer cell metabolism. Cancer Research 2009; 69:2163-2166.
84. Ryland L, Doshi U, Shanmugavelandy S, et al. C6-ceramide nanoliposomes target the Warburg effect in chronic lymphocytic leukemia. PLoS One 2013; 8:84648.
85. Zhou Y, Hileman EO, Plunkett W, et al. Free radical stress in chronic lymphocytic leukemia cells and its role in cellular sensitivity to ROS-generating anticancer agents. Blood. 2003;101(10):4098-4104.
86. Trachootham D, Alexandre J, Huang P. Targeting cancer cells by ROS-mediated mechanisms: a radical therapeutic approach? Nat Rev Drug Discov. 2009;8(7):579-591.
87. Carew JS, Nawrocki ST, Xu RH, et al. Increased mitochondrial biogenesis in primary leukemia cells: the role of endogenous nitric oxide and impact on sensitivity to fludarabine. Leukemia. 2004;18(12):1934-1940.
88. Tomic J, Lichty B, Spaner DE. Aberrant interferonsignaling is associated with aggressive chronic lymphocytic leukemia. Blood. 2011;117(9):2668-2680.
89. Wheeler ML, Defranco AL. Prolonged production of reactive oxygen species in response to B cell receptor stimulation promotes B cell activation and proliferation. J Immunol. 2012;189(9): 4405-4416.
90. Du¨hren-von Minden M, U¨ belhart R, Schneider D, et al. Chronic lymphocytic leukemia is driven by antigen-independent cell-autonomous signalling. Nature. 2012;489(7415):309-312.
91. Wu RP, Hayashi T, Cottam HB, et al. Nrf2 responses and the therapeutic selectivity of electrophilic compounds in chronic lymphocytic leukemia. Proc Natl Acad Sci USA. 2010;107(16): 7479-7484.
92. Frezza C, Gottlieb E. Mitochondria in cancer: Not just innocent bystanders. Seminars in Cancer Biology. 2009;19, 4-11.
93. Fantin VR, St-Pierre J, Leder P. Attenuation of LDH-A expression uncovers a link between glycolysis, mitochondrial physiology, and tumor maintenance. Cancer Cell. 2006;9(6):425–434.
94. Rossignol R, Gilkerson R, Aggeler R, et al. Energy substrate modulates mitochondrial structure and oxidative capacity in cancer cells. Cancer Res. 2004;64(3):985–993.
95. Bonnet S, Archer SL, Allalunis-Turner J, et al. A mitochondria-K+ channel axis is suppressed in cancer and its normalization promotes apoptosis and inhibits cancer growth. Cancer Cell. 2007;11(1):37–51.
96. Michelakis ED, Sutendra G, Dromparis P, et al. Metabolic modulation of glioblastoma with dichloroacetate. Sci Transl Med. 2010; 2: 31ra34.
97. Wong JY, Huggins GS, Debidda M, et al. Dichloroacetate induces apoptosis in endometrial cancer cells. Gynecol Oncol. 2008;109:394-402.

98. Cao W, Yacoub S, Shiverick KT, et al. Dichloroacetate (DCA) sensitizes both wild-type and over expressing Bcl-2 prostate cancer cells in vitro to radiation. Prostate. 2008;68:1223-1231.
99. Sun RC, Fadia M, Dahlstrom JE, et al. Reversal of the glycolytic phenotype by dichloroacetate inhibits metastatic breast cancer cell growth in vitro and in vivo. Breast Cancer Res Treat. 2010;120: 253-260.
100. Sun RC, Board PG, Blackburn AC. Targeting metabolism with arsenic trioxide and dichloroacetate in breast cancer cells. Mol Cancer. 2011; 10: 142.
101. Sanchez-Arago M, Chamorro M, Cuezva JM. Selection of cancer cells with repressed mitochondria triggers colon cancer progression. Carcinogenesis. 2010; 31: 567-576.
102. Tong J, Xie G, He J, et al. Synergistic antitumor effect of dichloroacetate in combination with 5-fluorouracil in colorectal cancer. J Biomed Biotechnol. 2011; 2011: 740564.
103. Ayyanathan K, Kesaraju S, Dawson-Scully K, et al. Combination of sulindac and dichloroacetate kills cancer cells via oxidative damage. PLoS One. 2012; 7: e39949.
104. Ishiguro T, Ishiguro M, Ishiguro R, et al. Cotreatment with dichloroacetate and omeprazole exhibits a synergistic antiproliferative effect on malignant tumors. Oncol Lett. 2012;3:726-728.
105. Sanchez WY, McGee SL, Connor T, et al. Dichloroacetate inhibits aerobic glycolysis in multiple myeloma cells and increases sensitivity to bortezomib. Br J Cancer. 2013;108:1624-1633.
106. Yeluri S, Madhok BM, Jayne DG. New Horizons in Cancer Therapy: Manipulating Tumour Metabolism. Biomed Res 2012; 23;17-23.
107. Sutendra G, Michelakis ED. Pyruvate dehydrogenase kinase as a novel therapeutic target in oncology. Front Oncol. 2013;7;3:38.
108. Fujiwara S, Kawano Y, Yuki H, et al. PDK1 inhibition is a novel therapeutic target in multiple myeloma. Br J Cancer. 2013;108:170-178.
109. Horn HF, Vousden KH. Coping with stress: multiple ways to activate p53. Oncogene. 2007;26, 1306–1316.
110. Mayo LD, Donner DB. The PTEN, Mdm2, p53 tumor suppressor-oncoprotein network. Trends Biochem. Sci. 2002;27, 462–467.
111. Augustyn KE, Merino EJ, Barton JK. A role for DNA-mediated charge transport in regulating p53: oxidation of the DNA-bound protein from a distance. Proc. Natl Acad. Sci. USA. 2007;104,18907–18912.
112. Karawajew L, Rhein P, Czerwony G, et al. Stress-induced activation of the p53 tumor suppressor in leukemia cells and normal lymphocytes requires mitochondrial activity and reactive oxygen species. Blood. 2005;105(12):4767-4775.
113. Lindstrom MS, Deisenroth C, Zhang Y. Putting a finger on growth surveillance: insight into MDM2 zinc finger-ribosomal protein interactions. Cell Cycle. 2007; 6, 434–437.
114. Zhao Y, Coloff JL, Ferguson EC, et al. Glucose metabolism attenuates p53 and Puma-dependent cell death upon growth factor deprivation. J. Biol. Chem. 2008;283, 36344–36353.
115. Bensaad K, Tsuruta A, Selak MA, et al. TIGAR, a p53-inducible regulator of glycolysis and apoptosis.

Cell. 2006;126, 107–120.

116. Stambolic V, MacPherson D, Sas D, et al. Regulation of PTEN transcription by p53. Mol. Cell . 2001;8, 317–325.
117. Mathupala SP, Heese C, Pedersen PL. Glucose catabolism in cancer cells. The type II hexokinase promoter contains functionally active response elements for the tumor suppressor p53. J. Biol. Chem. 1997;272, 22776–22780.
118. Kulawiec M, Ayyasamy V, Singh KK. P53 regulates mtDNA copy number and mitocheckpoint pathway. J. Carcinog. 2009;8, 8.
119. Okamura S, Ng CC, Koyama K, et al. Identification of seven genes regulated by wild-type p53 in a colon cancer cell line carrying a well-controlled wild-type p53 expression system. Oncol. Res. 1999;11, 281–285.
120. Matoba S, Kang JG, Patino WD, et al. p53 regulates mitochondrial respiration. Science. 2006;312, 1650-1653.
121. Bourdon A, Minai L, Serre V, et al. Mutation of RRM2B, encoding p53-controlled ribonucleotide reductase (p53R2), causes severe mitochondrial DNA depletion. Nature Genet. 2007;39, 776-780.
122. Burns DM, Richter JD. CPEB regulation of human cellular senescence, energy metabolism, and p53 mRNA translation. Genes Dev. 2008;22, 3449-3460.
123. Buzzai M, Jones RG, Amaravadi RK, et al. Systemic treatment with the antidiabetic drug metformin selectively impairs p53-deficient tumor cell growth. Cancer Res. 2007;67, 6745-6752.
124. Sablina AA, Budanov AV, Ilyinskaya GV, et al. The antioxidant function of the p53 tumor suppressor gene. Nature Med. 2005;11, 1306-1313.
125. Giannoni E, Buricchi F, Raugei G, et al. Intracellular reactive oxygen species activate Src tyrosine kinase during cell adhesion and anchorage-dependent cell growth. Mol. Cell. Biol. 2005;25,6391–6403.
126. Ramsey MR, Sharpless NE. ROS as a tumour suppressor? Nature Cell Biol. 2006;8,1213–1215.
127. Garrido C, Galluzzi L, Brunet M, et al. Mechanisms of cytochrome c release from mitochondria. Cell Death Differ. 2006;13, 1423-1433.
128. Vaughn AE., Deshmukh M. Glucose metabolism inhibits apoptosis in neurons and cancer cells by redox inactivation of cytochrome c. Nature Cell Biol. 2008;10, 1477–1483.
129. Schafer ZT, Grassian AR, Song L, et al. Antioxidant and oncogene rescue of metabolic defects caused by loss of matrix attachment. Nature. 2009;461,109–113.
130. Chen W, Sun Z, Wang XJ, et al. Direct interaction between Nrf2 and p21Cip1/WAF1 upregulates the Nrf2 mediated antioxidant response. Mol. Cell. 2009;34,663–673.
131. Vousden KH, Prives C. Blinded by the light: the growing complexity of p53. Cell. 200);137,413–431.
132. Hasegawa H, Yamada Y, Iha H, et al. Activation of p53 by Nutlin-3a, an antagonist of MDM2, induces apoptosis and cellular senescence in adult T-cell leukemia cells. Leukemia 2009;23;2090-2101.
133. Vassilev LT, Vu BT, Graves B, et al. In vivo activation of the p53 pathway by small-molecule antagonists

of MDM2. Science 2004;303:844-848.

134. Secchiero P, Barbarotto E, Tiribelli M, et al. Functional integrity of the p53-mediated apoptotic pathway induced by the nongenotoxic agent nutlin-3 in B-cell chronic lymphocytic leukemia (B-CLL). Blood 2006; 107:4122-4129.

135. Secchiero P, Melloni E, di Iasio MG, et al. Nutlin-3 up-regulates the expression of Notch1 in both myeloid and lymphoid leukemic cells, as part of a negative feedback antiapoptotic mechanism. Blood 2009; 113:4300-4308.

136. Zauli G, Voltan R, Bosco R, et al. Dasatinib plus Nutlin-3 shows synergistic antileukemic activity in both $p53^{wild\text{-}type}$ and $p53^{mutated}$ B chronic lymphocytic leukemias by inhibiting the Akt pathway. Clin. Cancer Res. 2011.

137. Zauli G, Celeghini C, Melloni E, et al. The sorafenib plus nutlin-3 combination promotes synergistic cytotoxicity in acute myeloid leukemic cells irrespectively of FLT3 and p53 status. Haematologica 2012;97:1722-1730.

138. Kumar A, Kant S, Singh SM. Novel molecular mechanisms of antitumor action of dichloroacetate against T cell lymphoma: Implication of altered glucose metabolism, pH homeostasis and cell survival regulation. Chem Biol Interact. 2012;199:29-37.

139. Secchiero P, Bosco R, Celeghini C, et al. Recent advances in the therapeutic perspectives in nutlin-3. Curr Pharm Des. 2011;17: 569-577.

140. Lin K, Adamson J, Johson GG, et al. Functional analysis of the ATM-p53-p21 pathway in the LRF CLL4 trial: blockade at the level of p21 is associated with short response duration. Clin Cancer Res. 2012;18: 4191-4200.

141. Zhang J, Li H, Yabut O, et al. Cdk5 suppresses the neuronal cell cycle by disrupting the E2F1-DP1 complex. J Neurosci. 2010 Apr 14;30(15):5219-5228.

142. Brunelli L, Llansola M, Felipo V, et al. Insight into the neuroproteomics effects of the food-contaminant non-dioxin like polychlorinated biphenyls. J Proteomics. 2012; 75: 2417-2430.

143. Sharaf el dein O, Mayola E, Chopineau J, et al. The adenine nucleotide translocase 2, a mitochondrial target for anticancer biotherapy. Curr Drug Targets. 2011;12(6):894-901.

144. Corthésy B, Kao PN. Purification by DNA affinity chromatography of two polypeptides that contact the NF-AT DNA binding site in the interleukin 2 promoter. J Biol Chem. 1994;269: 20682-20690.

145. Shi L, Zhao G, Qiu D, et al. NF90 regulates cell cycle exit and terminal myogenic differentiation by direct binding to the 3'-untranslated region of MyoD and p21WAF1/CIP1 mRNAs. J Biol Chem. 2005;280:18981-18989.

146. Karetsou Z, Sandaltzopoulos R, Frangou-Lazaridis M, et al. Prothymosin a modulates the interaction of histone H1 with chromatin. Nucleic Acids Res. 1998;26:3111–3118.

147. Kalo E, Kogan-Sakin I, Solomon H, et al. Mutant p53R273H attenuates the expression of phase 2 detoxifying enzymes and promotes the survival of cells with high levels of reactive oxygen species. J Cell Sci. 2012;125:5578-5586.

148. Kerr DS. Review of clinical trials for mitochondrial disorders: 1997-2012. Neurotherapeutics. 2013;10:307-319.
149. Chevrollier A, Loiseau D, Reynier P, et al. Adenine nucleotide translocase 2 is a key mitochondrial protein in cancer metabolism. Biochim Biophys Acta 2011;1807:562-567.
150. Yin F, Sancheti H, Cadenas E. Silencing of nicotinamide nucleotide transhydrogenase impairs cellular redox homeostasis and energy metabolism in PC12 cells. Biochim Biophys Acta 2012;1817:401-409.
151. Wu S, Huang S, Ding J, et al. Multiple microRNAs modulate p21Cip1/Waf1 expression by directly targeting its 3'-untranslated region. Oncogene. 2010;29:2302-2308.
152. Abbas T, Dutta A. p21 in cancer: Intricate networks and multiple activities. Nat Rev Cancer. 2009;9: 400-414.
153. Roninson IB. Oncogenic functions of tumor suppressor p21(Waf1/Cip1/Sdi1): Association with cell senescence and tumor-promoting activities of stromal fibroblasts. Cancer Lett. 2002;179: 1-14.
154. Gartel AL. The conflicting roles of the CDK inhibitor p21(CIP1/WAF1) in apoptosis. Leuk Res. 2005;29: 1237-1238.

List of publications in PhD

1. Agnoletto C, Brunelli L, Melloni E, Pastorelli R, Casciano F, Rimondi E, Rigolin GM, Cuneo A, Secchiero P, Zauli G. The anti-leukemic activity of sodium dichloroacetate in p53mutated/null cells is mediated by a p53-independent ILF3/p21 pathway. Oncotarget. 2014 Dec 10. [Epub ahead of print] [IF (2014)= 6.627]
2. Agnoletto C, Melloni E, Casciano F, Rigolin GM, Rimondi E, Celeghini C, Brunelli L, Cuneo A, Secchiero P, Zauli G. Sodium dichloroacetate exhibits anti-leukemic activity in B-chronic lymphocytic leukemia (B-CLL) and synergizes with the p53 activator Nutlin-3. Oncotarget. 2014 Jun 30;5(12):4347-60. [IF (2014)= 6.627]
3. Tisato V, Garrovo C, Biffi S, Petrera F, Voltan R, Casciano F, Meroni G, Agnoletto C, Zauli G, Secchiero P. Intranasal administration of recombinant TRAIL down-regulates CXCL-1/KC in an ovalbumin-induced airway inflammation murine model. PlosOne. 2014 Dec 15;9(12):e115387. [IF (2014)= 3.534]
4. Athanasakis E, Melloni E, Rigolin GM, Agnoletto C, Voltan R, Vozzi D, Piscianz E, Segat L, Dal Monego S, Cuneo A, Secchiero P, Zauli G. The p53 transcriptional pathway is preserved in ATMmutated and NOTCH1mutated chronic lymphocytic leukemias. Oncotarget. 2014 Dec 30;5(24):12635-45. [IF (2014)= 6.627]
5. Biffi S, Petrizza L, Rampazzo E, Voltan R, Sgarzi M, Garrovo C, Prodi L, Andolfi L, Agnoletto C, Zauli G, Secchiero P. Multiple dye-doped NIR-emitting silica nanoparticles for both flow cytometry and in vivo imaging. RSC Advances. 2014.4;18278-18285 [IF (2014)= 3.708]
6. Tornese G, Iafusco D, Monasta L, Agnoletto C, Tisato V, Ventura A, Zauli G, Secchiero P. The levels of circulating TRAIL at the onset of type 1 diabetes are markedly decreased in patients with ketoacidosis and with the highest insulin requirement. Acta Diabetol. 2014 Apr;51(2):239-46. [IF (2014)= 3.679]
7. Zauli G, Monasta L, Vecchi Brumatti L, Agnoletto C, Volpi P, Secchiero P. The circulating levels of TRAIL are extremely low after delivery but rapidly recover in both mothers and newborns. Cytokine. 2013 Oct;64(1):51-3. [IF (2013)= 2.874]
8. Secchiero P, Toffoli B, Melloni E, Agnoletto C, Monasta L, Zauli G. The MDM2 inhibitor Nutlin-3 attenuates streptozotocin-induced diabetes mellitus and increases serum level of IL-12p40. Acta Diabetol. 2013 Dec;50(6):899-906. [IF (2013)= 3.679]
9. Secchiero P, Rimondi E, di Iasio MG, Agnoletto C, Melloni E, Volpi I, Zauli G. C-Reactive protein downregulates TRAIL expression in human peripheral monocytes via an Egr-1-dependent pathway. Clin Cancer Res. 2013 Apr 15;19(8):1949-59. [IF (2013)= 8.193]